

An Online Meta-Level Adaptive-Design Framework with Targeted Learning Inference: Applications to Evaluating and Utilizing Surrogate Outcomes in Adaptive Designs

Wenxin Zhang¹, Aaron Hudson², Maya Petersen¹, Mark van der Laan¹ *

¹Division of Biostatistics, University of California, Berkeley

²Vaccine and Infectious Disease Division, Fred Hutchinson Cancer Center

November 14, 2025

Abstract

Adaptive designs are increasingly used in clinical trials and online experiments to improve participant outcomes by dynamically updating treatment allocation based on accumulating data. However, in practice, experimenters often consider multiple candidate designs, each with distinct trade-offs, while only one can be implemented at a time, leaving benefits and costs of alternative designs unobserved and unquantified. To address this, we propose a novel meta-level adaptive design framework that enables real-time, data-driven evaluation and selection among candidate adaptive designs. Specifically, we define a new class of causal estimands to evaluate adaptive designs, estimate them with Targeted Maximum Likelihood Estimation framework, which yields an asymptotically normal estimator accommodating dependence in adaptive-design data without parametric assumptions, and support online design selection. We further apply this framework to a motivating example where multiple surrogates of a long-term primary outcome are considered for updating randomization probabilities in adaptive experiments. Unlike existing surrogate evaluation methods, our approach comprehensively quantifies the utility of surrogates to accelerate detection of heterogeneous treatment effects, expedite updates to treatment randomization and improve participant outcomes, facilitating dynamic selection among surrogate-guided adaptive designs. Overall, our framework provides a unified tool for evaluating opportunities and costs of various adaptive designs and guiding real-time decision-making in adaptive experiments.

*This work was supported by NIAID award R01 AI074345. The content is solely the responsibility of the authors and does not necessarily represent the official views of the NIH. We gratefully acknowledge the contributions of the ADAPT-R Study Team (ClinicalTrials.gov number, NCT02338739) and Sponsor (National Institutes of Health grants R01 MH104123, K24 AI134413, and R01 AI074345).

1 Introduction

1.1 Overview

Adaptive experimental designs are gaining popularity in clinical trials and online experiments (Robertson et al., 2023; Larsen et al., 2024). Unlike traditional static experimental designs, adaptive designs allow continuous updates to treatment randomization probabilities and/or other experimental features based on accumulated data during the experiment, supporting a range of experimental objectives. Among the various benefits of adaptive designs, a key advantage is their ability to increase the probability of providing participants with their optimal treatment, particularly when this optimal treatment varies between individuals, thereby improving their outcomes.

However, in practice, experimenters often face the challenge of choosing among multiple candidate adaptive design configurations, each with its own trade-offs. A common and compelling example is an adaptive experiment with a longitudinal data structure, in which new participants are continuously enrolled and existing participants generate multiple short-term outcomes that unfold progressively over different follow-up times, while the primary outcome requires long-term follow-up. In such settings, surrogate outcomes, either the early proxies of the primary outcome or other relevant metrics requiring shorter follow-ups, have the potential to quickly identify more effective personalized treatments, inform timely adaptations of treatment randomization probabilities with sufficient data, and thereby enhance participants' welfare. However, when there are multiple candidate surrogates, choosing which surrogate to use in adaptive designs is governed by complex trade-offs. Early surrogates provide more abundant and timely data for rapid adaptation, but may be less accurate in detecting treatment effects relevant to the primary outcome. Later surrogates may offer more accurate guidance for optimal treatment, but their delayed availability and

limited data reduce their impact on early adaptation and participant benefit. In addition, the sensitivity with which a candidate surrogate captures heterogeneous treatment effects is a key driver of its utility: a surrogate that provides stronger signals for distinguishing which individuals benefit from which treatments enables more timely and targeted adaptation toward personalized treatment. Despite all these important factors, in practice, only one candidate adaptation can be implemented at each time point of the experiment. This constraint inevitably leaves the gains and losses of unchosen alternative designs unobserved and unquantified, and further complicates the challenge of navigating these trade-offs in a real-time experiment, underscoring the need for a rigorous statistical framework to overcome these difficulties.

To address these challenges, we propose an Online-Superlearner Adaptive-Design framework with Targeted Learning inference: a general and data-driven adaptive design system for real-time evaluation and dynamic selection among different candidate designs during ongoing adaptive experiments. We refer to this unified framework as TMLE-OSLAD, a Targeted Maximum Likelihood Estimation-based Online-Superlearner Adaptive Design, which itself constitutes a meta-level adaptive design. This framework comprises three key components, each making a distinct methodological contribution.

First, the proposed framework introduces a novel counterfactual perspective for adaptive experiments by asking: How might participants' outcomes have differed under alternative adaptive designs? To formalize this question, we define a new class of target estimands: the mean counterfactual primary outcome that would have been observed had each participant's treatment, beginning at their enrollment, been assigned according to treatment randomization functions specified by the candidate adaptive design.

Second, to enable valid inference from the non-i.i.d. data generated by adaptive experiments, we establish a Targeted Maximum Likelihood Estimation (TMLE) approach that yields a

consistent and asymptotically normal estimator without parametric assumptions, building upon martingale central limit theorems and equicontinuity results via maximal inequalities for martingale processes. We further leverage recent advances in higher-order Highly Adaptive Lasso ([van der Laan, 2023](#)) to provide equicontinuity conditions. These developments enable robust inference on the proposed causal estimand—the expected outcome under a candidate counterfactual adaptive design. At the end of the experiment, we also provide TMLEs for estimating other causal estimands of interest, such as the average treatment effect (ATE) and the mean outcome under optimal dynamic treatment regimes (rules) ([Murphy, 2003](#); [Robins, 2004](#); [van der Laan and Luedtke, 2015](#)).

Third, we introduce a TMLE-based Online-Superlearner adaptive design, which continuously updates estimates of the proposed estimand to evaluate and compare a library of candidate adaptive designs in real time, selects the data-driven best-performing design based on TMLE estimation and inference, dynamically adapts treatment randomization probabilities according to the chosen design, and continuously monitors and reevaluates the set of candidate designs throughout the experiment.

Returning to the motivating example of adaptive experiments involving surrogates, TMLE-OSLAD demonstrates an additional methodological advantage: it provides an adaptive-design perspective for rigorously quantifying the value of information flow as it unfolds over time and is continually leveraged to guide sequential decision-making. Specifically, TMLE-OSLAD enables, to the best of our knowledge, for the first time, a comprehensive causal estimand to evaluate the evolving surrogate utility in such settings with statistical inference. In this context, the target estimand is defined as the mean counterfactual primary outcome under a candidate surrogate-guided adaptive design - where each participant’s treatment randomization probability at enrollment is determined by the estimated conditional average treatment effect function of the surrogate outcome and adaptively tilted toward the estimated

optimal personalized treatment with the objective of optimizing the surrogate outcome. This metric comprehensively reflects all critical factors in accelerating participant benefit through sequential adaptive design, including the timeliness of surrogate availability for enabling early adaptation, its sensitivity to signal heterogeneous treatment effects, and its predictive accuracy for identifying the optimal personalized treatments for the primary outcome. This is in contrast to existing surrogate evaluation methods that are typically developed for static experimental settings without taking a dynamic, sequential decision-making perspective. Furthermore, our framework enables the principled, data-driven implementation of adaptive experiments by facilitating real-time evaluation and selection among different surrogate-guided adaptive designs to improve the primary outcome.

In summary, TMLE-OSLAD provides a comprehensive meta-level framework for monitoring and quantifying opportunities and costs across a library of candidate adaptive designs with diverse self-learning, adaptively responding algorithms, empowering data-driven, statistical-inference-based decision-making throughout the experiment, and is broadly generalizable to a wide range of adaptive experimental settings.

1.2 Related Work

Adaptive experimental designs. Adaptive design is an active research area in statistics. In clinical trials, adaptive design methods are useful due to their flexibility and efficiency (Chow and Chang, 2008). These designs enable adaptive modifications to key aspects such as eligibility criteria, randomization probabilities, and other design features based on sequentially accrued data. Among these, Response-Adaptive Randomization (RAR) updates treatment probabilities using treatment and outcome data of previously enrolled subjects to achieve estimation efficiency or enhance participant welfare by reducing assignment to inferior treatments (Hu and Rosenberger, 2006; Robertson et al., 2023). Covariate-Adjusted

Response-Adaptive (CARA) designs extend RAR by incorporating baseline covariates into randomization, enabling more personalized allocation and improved efficiency (Rosenberger et al., 2001; Hu and Rosenberger, 2006; Zhang et al., 2007; van der Laan, 2008; Rosenberger and Sverdlov, 2008; Atkinson et al., 2011; Cheung et al., 2014). One can also guide CARA for multiple objectives, e.g., by integrating both efficiency and ethics considerations in adaptation procedures (Hu et al., 2015), and by both balancing prognostic covariates and facilitating adaptation procedures using predictive covariates in CARA designs (Zhao et al., 2022). The origins of RAR and CARA also trace back to Thompson (1933) and Robbins (1952) and connect to multi-armed and contextual bandit literature (Bubeck et al., 2012; Lattimore and Szepesvári, 2020; Simchi-Levi and Wang, 2023). Our work differs by considering settings where multiple candidate adaptive designs are available to choose from and providing a principled way to navigate their trade-offs and select from these designs by TMLE-OSLAD framework, with applications to CARA designs with surrogate outcomes.

Surrogate outcomes. Surrogate outcomes are often considered as a substitute for the primary outcome when the primary outcome requires a long follow-up time or is expensive to measure. In clinical trials, using surrogate outcomes can result in earlier detection of treatment effects, accelerated drug approvals, and reduced costs (Buyse et al., 2000). Examples include vaccine-induced immune responses as endpoints for HIV protection (Gilbert and Hudgens, 2008) and predictive short-term metrics to facilitate digital experiments (Duan et al., 2021; Richardson et al., 2023). The use of surrogates when primary outcomes are delayed has also been discussed in the adaptive design literature (Robertson et al., 2023). Examples include using short-term responses to guide treatment allocation for outpatients with depressive disorder (Tamura et al., 1994) and for participants in stroke trials (Nowacki et al., 2017), Bayesian modeling of surrogate–primary relationships to support RAR designs (Huang et al., 2009), and contextual bandits that handle delayed rewards by running

pre-trained Bayesian reward models (McDonald et al., 2023) or constructing a surrogate outcome based on external data to impute the missing primary outcome (Yang et al., 2024). Gao et al. (2024) further analyzes RAR designs driven by an informative surrogate and provides consistent, asymptotically normal statistical inference for the primary outcome under exponential-family models. While these approaches implement RAR/CARA procedures under a specific surrogate-guided design, a unified framework is lacking to dynamically re-evaluate and select among multiple surrogates to guide adaptive experiments.

Another related research area is surrogate evaluation. Many statistical frameworks have been developed to evaluate surrogates (Prentice, 1989; Freedman et al., 1992; Robins and Greenland, 1992; Daniels and Hughes, 1997; Lin et al., 1997; Gilbert and Hudgens, 2008) and reviewed comprehensively (Buyse et al., 2000; VanderWeele, 2013; Weir and Taylor, 2022; Elliott, 2023). However, most do not account for the potential benefits and risks of using surrogate outcomes in adaptive randomized trials that aim to learn and respond to treatment effect heterogeneity. Navigating these trade-offs requires both novel approaches for quantifying the benefit of candidate surrogates, and novel designs and estimators that make possible online evaluation of these benefits and dynamic surrogate selection in response during the course of a study, which is addressed by our general TMLE-OSLAD framework.

Inference based on adaptive design data. The statistical inference procedure in TMLE-OSLAD is related to the problem of how to provide valid inference for adaptively collected data in the adaptive design literature. For example, Zhang et al. (2007) and Zhu (2015) established asymptotic results for making statistical inferences from data generated by CARA designs under some parametric models. Within the Targeted Maximum Likelihood Estimation framework (van der Laan and Rubin, 2006; van der Laan and Rose, 2011, 2018), van der Laan (2008) developed TMLE tailored to adaptive designs without relying on specific parametric assumptions; subsequent work employed TMLE to estimate risk

difference and log-relative risk (Chambaz and van der Laan, 2014) and the mean outcome under optimal treatment rules (Chambaz et al., 2017) in CARA designs. More recently, several works used stabilized doubly robust estimators, a class of approaches originally proposed by (Luedtke and van der Laan, 2016a) to provide inference for the mean outcome under a possibly non-unique optimal treatment strategy, to make valid inference to evaluate treatment effects or the mean outcome under a target treatment rule in multi-armed bandits (Hadad et al., 2021) and contextual bandits (Bibaut et al., 2021; Zhan et al., 2021). Our proposed target estimand, the mean outcome under counterfactual adaptive designs, is distinct from these methods and related to causal inference for time series (van der Laan and Malenica, 2018; Malenica et al., 2021, 2024). We develop a TMLE for this estimand and establish asymptotic normality by martingale theories and equicontinuity results. We also leverage properties of the càdlàg function classes (Gill et al., 1995) and non-parametric higher-order spline Highly Adaptive Lasso estimators (van der Laan, 2023) to establish the equicontinuity conditions.

The remainder of the paper is organized as follows. Section 2 introduces the statistical setup and the TMLE-OSLAD framework. Section 3 formalizes CARA with multiple surrogate outcomes. Section 4 provides the theoretical analysis. Section 5 presents simulation studies, followed by an extended real-data-based simulation in Section 6. Section 7 concludes.

2 TMLE-Based Online-Superlearner Adaptive Design

In this section, we outline the general data structure, notation, and methods for the proposed TMLE-OSLAD framework. Suppose we have a binary treatment $A \in \mathcal{A} = \{0, 1\}$ and baseline covariates $W \in \mathcal{W}$. Let Y_K denote the primary outcome, observed K follow-up periods after treatment assignment, with higher values indicating better outcomes. We also consider $K - 1$ intermediate surrogate outcomes Y_k , each observed at $k = 1, \dots, K - 1$.

Let T denote the total duration of enrollment in the adaptive experiment. At each time point, the experimenter uses historical data from previously enrolled participants to update the treatment assignment mechanism for the new participants. These updates can aim to increase the chance that participants will receive optimal personalized treatment by learning heterogeneous treatment effects, which are detailed in Section 3 and Appendix D.

2.1 Statistical Setup

Sequential data structure. We use $t = 1, \dots, T$ to index the sequential enrollment times when participants enter the study and are randomized to one of the treatment arms. Let $E(t)$ denote the number of subjects enrolled at time t , and define the cumulative enrollment by $N(t) = \sum_{t'=1}^t E(t')$. For each participant i , we sequentially observe $O_i = (t_i, W_i, A_i, Y_{i,1}, \dots, Y_{i,K})$, where t_i is the enrollment time, W_i are the baseline covariates observed at t_i , and A_i is the treatment assigned at t_i . Surrogate outcomes $Y_{i,1}, \dots, Y_{i,K-1}$ are observed at follow-up times $t_i + k$ for $k = 1, \dots, K - 1$. The final outcome of interest, $Y_{i,K}$, is observed at $t_i + K$. To emphasize the timeline when each variable becomes available, we define $\tilde{W}_i(t_i) \equiv W_i$, $\tilde{A}_i(t_i) \equiv A_i$, and $\tilde{Y}_i(t_i + k) \equiv Y_{i,k}$ for $k = 1, \dots, K$. We use these notations interchangeably. At each time t , the experimenter has access to all information accrued up to $t - 1$, denoted by $\bar{O}(t - 1) := \{\tilde{W}_i(t'), \tilde{A}_i(t'), \tilde{Y}_i(t') : i \in [N(t - 1)], t' \leq t - 1\}$. This represents all baseline covariates, treatments, and outcomes of previous participants that have become observable before time t . As time moves from $t - 1$ to t , we collect new data from two sets of participants: $\mathcal{I}_1(t) := \{i : t - K \leq t_i \leq t - 1\}$ and $\mathcal{I}_2(t) := \{i : t_i = t\}$. Here, $\mathcal{I}_1(t)$ contains previously enrolled participants whose outcomes are still arriving, and $\mathcal{I}_2(t)$ contains participants newly enrolled at time t . The experimenter first observes the outcomes revealed at time t for $\mathcal{I}_1(t)$, then updates the history $\bar{\mathcal{H}}(t) := \bar{O}(t - 1) \cup \{\tilde{Y}_i(t) : i \in \mathcal{I}_1(t)\}$, where $\tilde{Y}_i(t)$ is the outcome for participant i that becomes observable at time t . Next, the experimenter enrolls $\mathcal{I}_2(t)$, observes their baseline covariates, and assigns treatments.

Adaptive treatment randomization. When a new participant i is enrolled at time t_i , a treatment A_i can be randomized based on the information available up to that point and the baseline covariates W_i . We denote the participant-specific pre-treatment history as $\mathcal{H}(i) := (\overline{\mathcal{H}}(t_i), W_i)$, where $\overline{\mathcal{H}}(t_i)$ is the observed data of previous participants enrolled before time t_i . We assume that treatment randomization depends on a fixed-dimensional summary context of the history data before new participants' enrollment and their baseline covariates, defined as $C_i := f_C(\overline{\mathcal{H}}(t_i), W_i) \in \mathcal{C}$. The treatment randomization probability is generated by a mapping $g_i : \mathcal{C} \rightarrow \mathcal{G}$, where \mathcal{G} is a class of probability distributions of treatment assignment, and $g_i(a|C_i)$ is the probability of assigning $a \in \mathcal{A}$ given context C_i .

Likelihood. Let Q_W denote the distribution of baseline covariates W and Q_{Y_k} denote the distribution of Y_k given $W, A, Y_1, \dots, Y_{k-1}$ for outcome Y_k ($k = 1, \dots, K$). We assume for every participant i , $t_i \perp\!\!\!\perp (W_i, A_i, Y_{i,1}, \dots, Y_{i,k})$, $W_i \sim Q_W$, and $Y_{i,k} \sim Q_{Y_k}(\cdot | W_i, A_i, Y_{i,1}, \dots, Y_{i,k-1})$. Specifically, let q_W denote the marginal density of the baseline covariates W , and q_{Y_k} denote the conditional density of the k -th outcome Y_k given $W, A, Y_1, \dots, Y_{k-1}$. The likelihood of the observed data of n subjects is expressed by $p^n(o_1, \dots, o_n) = \prod_{i=1}^n q_W(w_i) g_i(a_i | C_i) \prod_{k=1}^K q_{Y_k}(y_{i,k} | w_i, a_i, y_{i,1}, \dots, y_{i,k-1})$.

Structural causal model. We formalize the data generating process through a structural causal model (SCM) (Pearl, 2000) over the experiment, which also underpins estimation and inference in our setting. At each time t , we first observe the history data $\overline{\mathcal{H}}(t)$, which includes, for previously enrolled participants with $t_i = t - k$ ($k = 1, \dots, K$), the outcomes given by $Y_{i,k} = f_{Y_k}(W_i, A_i, Y_{i,1}, \dots, Y_{i,k-1}, U_{Y_{i,k}})$. Second, for each new unit i enrolled at time t , we observe $t_i = t$; $W_i = f_W(U_{W_i})$; $C_i = f_C(W_i, \overline{\mathcal{H}}(t))$; and $A_i = f_A(C_i, U_{A_i})$. Here, $U_i = (U_{W_i}, U_{A_i}, U_{Y_{i,1}}, \dots, U_{Y_{i,K}})$ are exogenous variables independent across participants. The actual adaptive design for n subjects is represented by the sequence of applied treatment-randomization functions, denoted by $\mathbf{g}_{1:n} := \{g_i : i = 1, \dots, n\}$.

2.2 Evaluation of Counterfactual CARA Designs

Here we define a target estimand within a modified SCM under a counterfactual adaptive design. Consider an alternative adaptive design $\mathbf{g}_{*,1:n} := (g_{*,1}, \dots, g_{*,n})$. For every i , we replace $A_i = f_A(C_i, U_{A_i})$ in the original SCM with $A_i^* \sim g_{*,i}(\cdot | C_i)$, which is a treatment randomization function based on the observed summary measure C_i at the time of entry, under the adaptive design $\mathbf{g}_{*,1:n}$. Consequently, the outcomes follow $Y_{i,k}^* = f_{Y_k}(W_i, A_i^*, Y_{i,1}^*, \dots, Y_{i,k-1}^*, U_{Y_{i,k}})$ for $k = 1, \dots, K$. Define $\bar{C}(n) := (C_1, \dots, C_n)$. Under the modified SCM, we propose the following target estimand:

$$\Psi_{\mathbf{g}_{*,1:n}}(\bar{C}(n)) = \frac{1}{n} \sum_{i=1}^n E_{g_{*,i}(\cdot | C_i)} [Y_{i,K}^*],$$

the mean counterfactual primary outcome had all participants, at their entry, been treated according to the treatment randomization mechanism $g_{*,i}$ that could have been applied under the alternative adaptive design $\mathbf{g}_{*,1:n}$.

This target estimand naturally supports the counterfactual evaluation of multiple candidate adaptive designs of interest. Suppose we have J different candidate adaptive designs, where each design is defined by a series of counterfactual treatment randomization functions $\{g_{j,i}^* : i = 1, \dots, n\}$ for $j \in [J]$, and depends on the j -specific design configuration aiming to increase the probability that new participants receive personalized optimal treatment assignments to maximize their outcomes. The corresponding counterfactual estimand for the j -th candidate design is defined as: $\Psi_j := \frac{1}{n} \sum_{i=1}^n E_{g_{j,i}^*(\cdot | C_i)} [Y_{i,K}^*]$, reflecting the expected final outcome had the population been treated under that adaptive design. This enables a principled comparison of all candidate designs by comparing the values of $\{\Psi_j\}_{j=1}^J$.

Let $Q_0 := (Q_{0,W}, Q_{0,K}) \in \mathcal{Q}_W \times \mathcal{Q}_K$, where $Q_{0,W}$ is the true distribution of W , and $Q_{0,K}$ is the conditional distribution of Y_K given A and W , with the associated $\bar{Q}_{0,K}$ denoting the

true conditional mean function of the final outcome Y_K given A and W . We also use $g_{0,i}$ to denote the actual treatment randomization function applied to each participant i in the experiment, which is known to the experimenter. One can identify the proposed causal estimand based on the observed data under the following assumptions.

Assumption 1 (Sequential Exchangeability). *For any $i \in [n]$, $Y_{i,K}(a) \perp\!\!\!\perp A_i \mid C_i$.*

Assumption 2 (Positivity). *For any $i \in [n]$ and $a \in \mathcal{A}$, $g_{0,i}(a|C_i) > 0$.*

Theorem 1 (Identification). *With assumptions 1 and 2, one can identify Ψ_j under Q_0 by*

$$\Psi_j(Q_0) = \Psi_{\mathbf{g}_{j,1:n}^*}(Q_0) = \frac{1}{n} \sum_{i=1}^n E_{Q_0, g_{j,i}^*} [Y_{i,K}^*] = \frac{1}{n} \sum_{i=1}^n \sum_{a=0}^1 \bar{Q}_{0,K}(a, W_i) g_{j,i}^*(a|C_i).$$

We note that this estimand provides a fast and robust approximation to an ideal estimand: the expected outcome obtained by integrating the entire distribution of data that would sequentially arise from the candidate adaptive design of interest. However, the latter’s estimation is considerably more complex and computationally intensive. In contrast, our proposed context-specific estimand substantially simplifies the estimation procedure, enables doubly-robust estimation, and closely approximates the ideal estimand when the observed contexts are reflective of those that would be observed in the candidate design, especially when the adaptation procedure is based on learning from a stationary target (e.g. Q_0) that dominates over the experiments. This yields an efficient and effective approach to distinguishing high-performing from low-performing designs and facilitating online selection among candidate designs. We refer readers to Appendix A.2 for further discussions and empirical results showing minimal difference between the two estimands in our simulations.

2.3 Targeted Maximum Likelihood Estimation

At each time point t , let $n_t := N(t - K)$ denote the total number of participants for whom the final outcome Y_K has been observed at that time. We define the target estimand for the j -th counterfactual adaptive design at time t as

$$\Psi_{t,j} := \frac{1}{n_t} \sum_{i=1}^{n_t} E_{Q_{0,g_{j,i}^*}} [Y_{i,K}^*] = \frac{1}{n_t} \sum_{i=1}^{n_t} \sum_{a=0}^1 \bar{Q}_{0,K}(a, W_i) g_{j,i}^*(a|C_i).$$

To estimate $\Psi_{t,j}$, we provide a Targeted Maximum Likelihood Estimation (TMLE) approach. Let $\bar{Q}_{n,K,t}$ be an initial estimate of $\bar{Q}_{0,K}$ based on the historical data $\bar{\mathcal{H}}(t)$ observed up to time t . We apply a TMLE procedure to update $\bar{Q}_{n,K,t}$ by fitting the logistic model (van der Laan and Rubin, 2006; van der Laan, 2008; van der Laan and Rose, 2011; Malenica et al., 2024): $\text{logit } \bar{Q}_{n,K,t,\epsilon}(A, W) = \text{logit } \bar{Q}_{n,K,t}(A, W) + \epsilon$, with weights $\frac{g_{j,i}^*(A_i|C_i)}{g_{0,i}(A_i|C_i)}$. The estimate of ϵ is denoted by $\hat{\epsilon}_t$, and an updated estimator of the conditional mean function $\bar{Q}_{n,K,t}^* := \bar{Q}_{n,K,t,\hat{\epsilon}_t}$ is obtained, which solves: $\frac{1}{n_t} \sum_{i=1}^{n_t} \frac{g_{j,i}^*(A_i|C_i)}{g_{0,i}(A_i|C_i)} (Y_{i,K} - \bar{Q}_{n,K,t}^*(A_i, W_i)) = 0$. The TMLE estimate of $\Psi_{t,j}$ is:

$$\hat{\Psi}_{t,j} := \frac{1}{n_t} \sum_{i=1}^{n_t} \sum_{a=0}^1 \bar{Q}_{n,K,t}^*(a, W_i) g_{j,i}^*(a|C_i).$$

The estimated standard error is $\sqrt{\hat{\sigma}_{t,j}^2/n_t}$, where $\hat{\sigma}_{t,j}^2 := \frac{1}{n_t} \sum_{i=1}^{n_t} \left[\frac{g_{j,i}^*(A_i|C_i)}{g_{0,i}(A_i|C_i)} (Y_{i,K} - \bar{Q}_{n,K,t}^*(A_i, W_i)) \right]^2$. The $100(1-\alpha)\%$ Wald confidence interval for $\hat{\Psi}_{t,j}$ is $\left[\hat{\Psi}_{t,j} - z_{1-\alpha/2} \sqrt{\frac{1}{n_t} \hat{\sigma}_{t,j}^2}, \hat{\Psi}_{t,j} + z_{1-\alpha/2} \sqrt{\frac{1}{n_t} \hat{\sigma}_{t,j}^2} \right]$, where $z_{1-\alpha/2}$ is the $1 - \alpha/2$ quantile of the standard normal distribution (e.g. $\alpha = 0.05$).

As shown in Section 4, TMLE is consistent, asymptotically normal, and doubly robust, meaning it remains consistent if either the outcome regression or the treatment assignment mechanism is correctly specified. Since the true assignment mechanism is known by adaptive design, consistency holds even if the outcome regression is misspecified. We also note that,

on top of its doubly robust property, obtaining a more accurate estimate of the conditional outcome function $\bar{Q}_{0,K}$ helps reduce the variance of TMLE. When there is flexibility in how to estimate $\bar{Q}_{0,K}$, a Super Learner (van der Laan et al., 2007) can be applied to select the best-performing estimator through cross-validation. We also suggest including the higher-order Highly Adaptive Lasso (van der Laan, 2023) in the Super Learner library for estimating $\bar{Q}_{0,K}$ to facilitate equicontinuity conditions underlying these theoretical properties.

2.4 Online-Superlearner Adaptive Design

As the experiment progresses to a new time point t , there are up to J candidate treatment randomization functions $g_{1,i}^*, \dots, g_{J,i}^*$ for assigning treatment randomization probabilities for a new participant i enrolled at t . For each $j \in [J]$, $g_{j,i}^*$ is generated based on historical data using the j -specific adaptive design configurations. The proposed Online-Superlearner Adaptive Design begins by estimating $\Psi_{t,j}$ for each $j \in [J]$ and obtaining confidence intervals for these estimates. Then, it selects the design indexed by $j_t^* := \operatorname{argmax}_{j \in [J]} \hat{\Psi}_{t,j} - z_{1-\alpha/2} \sqrt{\frac{1}{n_t} \hat{\sigma}_{t,j}^2}$, the candidate design with the highest lower confidence interval bound among all $\hat{\Psi}_{t,j}$ for $j \in [J]$, prioritizing high-performing designs with low uncertainty to mitigate the risk of selecting a suboptimal design due to unstable estimates. Finally, for all participants i enrolled at time t , we assign treatment randomization probabilities using $g_{j_t^*,i}^*$.

2.5 Statistical Inference at the End of Adaptive Experiments

We use $T_{end} := T + K$ to denote the time when the entire experiment ends, that is, the time point once all final outcomes Y_K have been observed after the last enrollment at time T . The total sample size at this point is denoted by $n_{end} := N(T) = \sum_{t=1}^T E(t)$, representing the total number of participants enrolled up to time T . At this final time point, one can

follow the same methodology outlined in Section 2.3 to estimate $\Psi_{T_{end},j}$, which represents the expected final outcome under the j -th counterfactual adaptive design. Beyond this, we also provide TMLEs for other causal estimands commonly studied in randomized trials, such as the average treatment effect and the mean outcome under dynamic treatment rules.

Average treatment effect. One can define the following average treatment effect (ATE) on the primary outcome Y_K across all participants within the experiment:

$\psi_{K,T_{end}}^{\text{ATE}} := \frac{1}{n_{end}} \sum_{i=1}^{n_{end}} [\bar{Q}_{0,K}(1, W_i) - \bar{Q}_{0,K}(0, W_i)]$. This can be estimated by first obtaining an initial estimator $\bar{Q}_{n,K,T_{end}}$ for the conditional mean function $\bar{Q}_{0,K}$ using all data across the experiment, then applying the TMLE procedure to solve $\frac{1}{n_{end}} \sum_{i=1}^{n_{end}} \frac{2A_i-1}{g_{0,i}(A_i|C_i)} (Y_{i,K} - \bar{Q}_{n,K,T_{end}}^*(A_i, W_i)) = 0$. The TMLE estimate of $\psi_{K,T_{end}}^{\text{ATE}}$ is $\hat{\psi}_{K,T_{end}}^{\text{ATE}} := \frac{1}{n_{end}} \sum_{i=1}^{n_{end}} [\bar{Q}_{n,K,T_{end}}^*(1, W_i) - \bar{Q}_{n,K,T_{end}}^*(0, W_i)]$. The standard error is given by $\sqrt{\hat{\sigma}_{K,T_{end}}^{2,\text{ATE}}/n_{end}}$, where $\hat{\sigma}_{K,T_{end}}^{2,\text{ATE}} = \frac{1}{n_{end}} \sum_{i=1}^{n_{end}} \left[\frac{2A_i-1}{g_{0,i}(A_i|C_i)} (Y_{i,K} - \bar{Q}_{n,K,T_{end}}^*(A_i, W_i)) \right]^2$.

Mean outcome under a dynamic treatment rule. Let $d : \mathcal{W} \rightarrow \mathcal{A}$ denote a fixed dynamic treatment rule that maps baseline covariates to a certain treatment arm. We then

define the target estimand $\psi_d := \frac{1}{n_{end}} \sum_{i=1}^{n_{end}} \bar{Q}_{0,K}(d(W_i), W_i)$ as the mean final outcome Y_K that would be obtained had treatments been assigned according to the dynamic treatment rule d . By solving $\frac{1}{n_{end}} \sum_{i=1}^{n_{end}} \frac{I(A_i=d(W_i))}{g_{0,i}(A_i|C_i)} (Y_{i,K} - \bar{Q}_{n,K,T_{end}}^*(A_i, W_i)) = 0$, the TMLE estimate of ψ_d is $\hat{\psi}_d = \frac{1}{n_{end}} \sum_{i=1}^{n_{end}} \bar{Q}_{n,K,T_{end}}^*(d(W_i), W_i)$. The estimated standard error is $\sqrt{\hat{\sigma}_d^2/n_{end}}$, where $\hat{\sigma}_d^2 := \frac{1}{n_{end}} \sum_{i=1}^{n_{end}} \left[\frac{I(A_i=d(W_i))}{g_{0,i}(A_i|C_i)} (Y_{i,K} - \bar{Q}_{n,K,T_{end}}^*(A_i, W_i)) \right]^2$.

3 Evaluating and Utilizing Surrogates in CARA Designs

In this section, we apply the general TMLE-OSLAD framework to the motivating example of adaptive experiments involving multiple surrogate outcomes before the final outcome. Recall

that there are $K - 1$ candidate surrogate outcomes, Y_1, \dots, Y_{K-1} , each measured prior to the final primary outcome Y_K at follow-up times $k = 1, \dots, K - 1$. Each surrogate Y_k defines a distinct candidate adaptive design, which leverages accumulating information from short-term surrogate outcomes to increase the probability for assigning the estimated personalized treatment associated with that surrogate over time. TMLE-OSLAD is implemented to continuously evaluate and dynamically select among different surrogate-specific adaptive designs over the experiment. We first introduce a CARA procedure to adapt treatment randomization probabilities aiming to improve participant outcomes by increasing the assignment of the estimated optimal personalized treatment based on conditional average treatment effect (CATE). Building upon the framework in Section 2, we define our target estimand that evaluates each candidate surrogate within a counterfactual adaptive design that utilizes the surrogate to adapt treatment randomization probabilities. We will also demonstrate how to use the TMLE to estimate these target estimands to evaluate surrogates, and introduce the TMLE-OSLAD adaptive design to evaluate different surrogates and utilize the most useful one to guide the ongoing adaptive experiment. Finally, we provide methods to conduct post-experiment inference for other causal estimands in this context.

3.1 CARA Designs Using Surrogate Outcomes

In our CARA designs, at each time point, we update the model to estimate the CATE for the outcome of interest and its associated uncertainty, and use these estimates to assign randomization probabilities to newly enrolled participants. This design aims to maximize participant outcomes by increasing the chance to allocate the estimated optimal treatment, with a principled exploration–exploitation balance ensuring sufficient exploration when the superiority of a treatment arm is uncertain and maintaining the ability to continue learning heterogeneous treatment effect from data collected at later time points. Specifically, when the estimated CATE is small relative to its uncertainty, indicating that the superiority of one

treatment arm is uncertain, the treatment randomization probabilities remain close to 0.5. This avoids overcommitting to a noisy and potentially suboptimal rule and ensures sufficient exploration across treatment arms. As the estimated CATE suggests a stronger signal for the superior treatment arm, the probability of assigning that treatment increases up to a maximum exploitation probability. Meanwhile, a positive lower bound on the probability of assigning the alternative arm is maintained to ensure sufficient support for valid estimation and inference of other estimands at the end of the experiment (see Sections 2.5 and 3.3).

More details of the CARA design are provided in the Appendix. Specifically, CATE is estimated using a doubly robust approach based on pseudo-outcomes (van der Laan, 2006; Luedtke and van der Laan, 2016b) (Appendix C), with point estimates and confidence intervals constructed based on higher-order Highly Adaptive Lasso (HAL) (van der Laan, 2023) (Appendix B). Details of the treatment randomization function can be found in Appendix D.

3.2 Surrogate-Guided Online-Superlearner Adaptive Design

To enable data-adaptive selection of the most effective surrogate to guide treatment allocation, we leverage the general TMLE-OSLAD framework in Section 2 to both evaluate and dynamically utilize candidate surrogate outcomes within real-time CARA experiments. At each interim time t , we use all observed historical data to assess the utility of each surrogate-driven adaptive design and to select the most promising surrogate for adaptation.

First, at time t , we define the target estimand $\Psi_{t, \mathbf{g}_{k,1:n_t}^*} := \frac{1}{n_t} \sum_{i=1}^{n_t} E_{g_{k,i}^*} [Y_{i,K}^*]$ for each candidate surrogate Y_k , which represents the mean final outcome that would be achieved for the n_t fully-followed participants if each had been assigned with the treatment randomization function $g_{k,i}^*$, at their enrollment, determined by the adaptive design using surrogate Y_k . We refer to this estimand as “the utility of a surrogate” in the CARA design.

Since the construction of $g_{k,i}^*$ relies on the estimated CATE for Y_k based on the accumulated data, we require the following sequential exchangeability assumption to estimate CATE.

Assumption 3 (Sequential Exchangeability for Surrogate Outcomes). *For any $k \in \{1, \dots, K-1\}$ and any subject $i \in \{1, \dots, n_t\}$, $Y_{i,k}(a) \perp\!\!\!\perp A_i \mid C_i$.*

In conjunction with Assumptions 1 and 2, $\Psi_{t, \mathbf{g}_{k,1:n_t}^*}$ can be identified as $\Psi_{t,k} := \frac{1}{n_t} \sum_{i=1}^{n_t} \sum_{a=0}^1 \bar{Q}_{0,K}(a, W_i) g_{k,i}^*(a|C_i)$. Then, we estimate $\Psi_{t,k}$ for each surrogate Y_k using TMLE, which is given by $\hat{\Psi}_{t,k} = \frac{1}{n_t} \sum_{i=1}^{n_t} \sum_{a=0}^1 \bar{Q}_{n,K,t}^*(a, W_i) g_{k,i}^*(a|C_i)$. The estimated standard error is $\sqrt{\hat{\sigma}_{t,k}^2/n_t}$, where $\hat{\sigma}_{t,k}^2 = \frac{1}{n_t} \sum_{i=1}^{n_t} \left[\frac{g_{k,i}^*(A_i|C_i)}{g_{0,i}(A_i|C_i)} \left(Y_{i,K} - \bar{Q}_{n,K,t}^*(A_i, W_i) \right) \right]^2$. Next, we compare all candidate surrogates and the final outcome by constructing confidence intervals for $\Psi_{t,k}$'s ($k = 1, \dots, K$) and identify the outcome $Y_{k_t^*}$ with the highest lower confidence bound, where $k_t^* := \operatorname{argmax}_{k \in [K]} \hat{\Psi}_{t,k} - z_{1-\alpha/2} \sqrt{\hat{\sigma}_{t,k}^2/n_t}$. For example, if two surrogates have similar point estimates but one yields a much narrower confidence interval, the surrogate with the higher lower bound is prioritized, as it reflects more evidence in its utility relative to uncertainty. Accordingly, we select $Y_{k_t^*}$ as the outcome to guide the next-stage treatment assignment for newly enrolled participants at time t , utilizing the treatment randomization function $g_{k_t^*,i}^*$. This procedure is repeated at each subsequent time point, allowing adaptive surrogate selection and treatment allocation as new data accrue.

3.3 Inference after Adaptive Experiments Involving Surrogates

At the end of the adaptive experiment, one can follow Section 2.5 to conduct statistical inference for various causal estimands, such as the average treatment effect and the mean outcome under dynamic treatment rules. Here, we briefly discuss how to estimate the mean primary outcome under optimal treatment rules (OTR) that maximize the expected primary outcome (Murphy, 2003; Robins, 2004; van der Laan and Luedtke, 2015) or a surrogate outcome (Hsu et al., 2015; Yang et al., 2024). Specifically, for any outcome Y_k

($k \in \{1, \dots, K\}$), one can consider the optimal treatment rule $d_{0,k}^* : \mathcal{W} \rightarrow \mathcal{A}$, defined by $d_{0,k}^*(W) = I(E[Y_k(1) - Y_k(0)|W] > 0)$. This rule assigns the treatment that maximizes the expected value of Y_k given the baseline covariates. At the end of the experiment, we learn this rule using the observed data and obtain an estimated rule $d_{n,k,T_{end}}^* : \mathcal{W} \rightarrow \mathcal{A}$. The corresponding target estimand for the mean primary outcome under that estimated optimal rule is $\psi_{d_{n,k,T_{end}}^*} = \frac{1}{n_{end}} \sum_{i=1}^{n_{end}} \bar{Q}_{0,K}(d_{n,k,T_{end}}^*(W_i), W_i)$. We note that for $d_{n,K,T_{end}}^*$, i.e., the estimated optimal treatment rule trained to maximize the primary outcome Y_K itself, the standard TMLE estimate of the mean primary outcome under this rule may exhibit upward bias because the same data are used both to learn the rule and to estimate the expected outcome under that rule. We recommend applying cross-validated TMLE (CV-TMLE) (Zheng and van der Laan, 2011; van der Laan and Luedtke, 2015; Montoya et al., 2021) which uses sample splitting to avoid finite sample bias.

4 Theoretical Analysis of TMLE

This section derives consistency and asymptotic normality of the proposed TMLE. For notational continuity with the surrogate-guided adaptive design setup introduced above, we continue to index candidate designs by $k \in [K]$ in the TMLE analysis, and the target estimand of interest is $\Psi_{t,k}$. This indexing is notationally equivalent to the general index $j \in [J]$ used in Section 2 for estimating $\Psi_{t,j}$; the theoretical results and proofs apply identically under either notation. We first study the difference of TMLE $\hat{\Psi}_{t,k}$ and the truth $\Psi_{t,k}$. For any $\bar{Q}_K \in \bar{\mathcal{Q}}_K$, define $D_k(\bar{Q}_K)(O_i, C_i) := \frac{g_{k,i}^*(A_i|C_i)}{g_{0,i}(A_i|C_i)} (Y_{i,K} - \bar{Q}_K(A_i, W_i))$.

Theorem 2. *For any $\bar{Q}_{n,K,t}^* \in \bar{\mathcal{Q}}_K$ and $\bar{Q}_{1,K} \in \bar{\mathcal{Q}}_K$, the difference between $\hat{\Psi}_{t,k}$ and $\Psi_{t,k}$ can be decomposed as $\hat{\Psi}_{t,k} - \Psi_{t,k} = M_{1,n_t}(\bar{Q}_{1,K}) + M_{2,n_t}(\bar{Q}_{n,K,t}^*, \bar{Q}_{1,K})$, where*

$$M_{1,n_t}(\bar{Q}_{1,K}) = \frac{1}{n_t} \sum_{i=1}^{n_t} \left[D_k(\bar{Q}_{1,K})(O_i, C_i) - E \left[D_k(\bar{Q}_{1,K})(O_i, C_i) | \mathcal{H}(i) \right] \right],$$

$$M_{2,n_t}(\bar{Q}_{n,K,t}^*, \bar{Q}_{1,K}) = \frac{1}{n_t} \sum_{i=1}^{n_t} \left\{ \left[D_k(\bar{Q}_{n,K,t}^*)(O_i, C_i) - E[D_k(\bar{Q}_{n,K,t}^*)(O_i, C_i) | \mathcal{H}(i)] \right] \right. \\ \left. - \left[D_k(\bar{Q}_{1,K})(O_i, C_i) - E[D_k(\bar{Q}_{1,K})(O_i, C_i) | \mathcal{H}(i)] \right] \right\}.$$

The difference of TMLE $\hat{\Psi}_{t,k}$ and the true $\Psi_{t,k}$ is decomposed into M_{1,n_t} , an average of a martingale difference sequence, and a martingale process M_{2,n_t} . Under the strong positivity and stabilized conditional variance conditions below, the asymptotic normality of M_{1,n_t} follows directly from the martingale central limit theorem (e.g., Theorem 2 in [Brown \(1971\)](#)).

Assumption 4 (Strong positivity). *For any i , there exists $\zeta > 0$ such that $g_{0,i} > \zeta$ and $g_{k,i}^* > \zeta$.*

Assumption 5 (Stabilization of the average of conditional variances). *There exists $\sigma_{t,k}^2 \in \mathbb{R}^+$ such that $\frac{1}{n_t} \sum_{i=1}^{n_t} \text{Var}[D_k(\bar{Q}_{1,K})(O_i, C_i) | \mathcal{H}(i)] \xrightarrow{p} \sigma_{t,k}^2$.*

Theorem 3 (Asymptotic normality of the first term). *Suppose that assumptions 4 and 5 hold, then $\sqrt{n_t} M_{1,n_t}(\bar{Q}_{1,K}) \xrightarrow{d} N(0, \sigma_{t,k}^2)$.*

We note that M_{1,n_t} depends only on a fixed function $\bar{Q}_{1,K} \in \bar{\mathcal{Q}}_K$. Importantly, to obtain the asymptotic normality of the TMLE, $\bar{Q}_{1,K}$ need not equal the true conditional mean $\bar{Q}_{0,K}$ as long as $\bar{Q}_{n,K,t}^*$ converges to $\bar{Q}_{1,K}$ in a way that satisfies the equicontinuity condition for the second term, M_{2,n_t} , as formalized below.

Assumption 6 (Entropy integral of $\bar{\mathcal{Q}}_K$). *Let $N_\infty(\epsilon, \bar{\mathcal{Q}}_K)$ denote the ϵ -covering number in supremum norm of $\bar{\mathcal{Q}}_K$. Define $J_\infty(\epsilon, \bar{\mathcal{Q}}_K) := \int_0^\epsilon \sqrt{\log(1 + N_\infty(u, \bar{\mathcal{Q}}_K))} du$ as the ϵ -entropy integral in supremum norm of $\bar{\mathcal{Q}}_K$. Assume that $J_\infty(\epsilon, \bar{\mathcal{Q}}_K)$ is finite and $J_\infty(\epsilon, \bar{\mathcal{Q}}_K) \rightarrow 0$ as $\epsilon \rightarrow 0$.*

Assumption 7 (Convergence of $\bar{Q}_{n,K,t}^*$). For any $\bar{Q}_K \in \bar{\mathcal{Q}}_K$, define

$$s_{n_t}(\bar{Q}_K, \bar{Q}_{1,K}) := \sqrt{\frac{1}{n_t} \sum_{i=1}^{n_t} E \left[\phi \left(\frac{|D_k(\bar{Q}_K)(O_i, C_i) - D_k(\bar{Q}_{1,K})(O_i, C_i)|}{v} \right) \mid C_i \right]},$$

where $\phi(x) := e^x - x - 1$, $v := 8(1 - \zeta)/\zeta$. Assume that $s_{n_t}(\bar{Q}_{n,K,t}^*, \bar{Q}_{1,K}) = O_P(\delta_{n_t})$ for some $\delta_{n_t} \rightarrow 0$.

Theorem 4 (Equicontinuity). Under Assumptions 4, 6, and 7, $M_{2,n_t}(\bar{Q}_{n,K,t}^*, \bar{Q}_{1,K}) = o_P\left(n_t^{-\frac{1}{2}}\right)$.

This equicontinuity result demonstrates that, in addition to the asymptotic normality of M_{1,n_t} , the remainder term M_{2,n_t} is negligible. The proof is given in Appendix F, which depends on the equicontinuity result of the martingale process in general setup with sequential dependence (Appendix E). We further provide a sufficient way to satisfy the equicontinuity condition by leveraging the recent work of [van der Laan \(2023\)](#) that introduces a class of m -th order smoothness class of functions with m -th-order Radon-Nikodym derivative w.r.t. Lebesgue measure is càdlàg and of bounded variation ($m = 1, 2, \dots$), along with a higher-order spline Highly Adaptive Lasso (HAL) estimator (see Appendix B). We show that if $\bar{Q}_{n,K,t}$ is estimated by higher-order HAL and converges to a $\bar{Q}_{1,K}$ that is in the same class of functions, then the equicontinuity condition holds (see Appendix F).

Assumption 8. $\bar{Q}_{1,K}$ and $\bar{Q}_{n,K,t}$ are both from a class of functions that are represented by an m -th order smooth function whose m -th order Radon-Nikodym derivatives are càdlàg functions with bounded sectional variation norm ($m = 1, 2, \dots$), and $\bar{Q}_{n,K,t}$ is obtained by the m -th order Highly Adaptive Lasso estimator.

Corollary 1. Suppose Assumptions 4 and 8 hold. Then $M_{2,n_t}(\bar{Q}_{n,K,t}^*, \bar{Q}_{1,K}) = o_P\left(n_t^{-\frac{1}{2}}\right)$.

Theorem 5 (Asymptotic normality of TMLE). Suppose Assumptions 4, 5, 6, and 7 hold,

or alternatively, Assumptions 4, 5, and 8 hold, then $\sqrt{n_t}(\hat{\Psi}_{t,k} - \Psi_{t,k}) \xrightarrow{d} N(0, \sigma_{t,k}^2)$.

The asymptotic normality of TMLE is obtained directly from Theorems 3 and 4. We estimate the standard error by $\hat{\sigma}_{t,k}^2 := \frac{1}{n_t} \sum_{i=1}^{n_t} \left\{ \frac{g_{k,i}^*(A_i|C_i)}{g_{0,i}(A_i|C_i)} [Y_{i,K} - \bar{Q}_{n,K,t}^*(A_i, W_i)] \right\}^2$ (which converges in probability to $\sigma_{t,k}^2$), with the confidence interval $[\hat{\Psi}_{t,k} - z_{1-\alpha/2} \sqrt{\hat{\sigma}_{t,k}^2/n_t}, \hat{\Psi}_{t,k} + z_{1-\alpha/2} \sqrt{\hat{\sigma}_{t,k}^2/n_t}]$.

5 Simulation Studies

Simulation setup. We present simulation studies to evaluate the performance of our proposed adaptive design and estimation methods. We consider a binary treatment $A \in \{0, 1\}$, a univariate baseline covariate W following a uniform distribution $U(-4, 4)$, four surrogate outcomes Y_k measured at follow-up times $k = 1, 2, 3, 4$, respectively, and a final outcome Y_5 . Each participant's outcome Y_k is generated by its conditional mean $E(Y_k|A, W)$ plus a random error following the normal distribution ($\sim N(0, 1)$). For detailed information on the simulations, we refer readers to Appendix C for CATE estimation, Appendix D for treatment randomization mechanism and Appendix G for data generating distributions.

We evaluate the performance of various designs in two scenarios. In Scenario 1 (Figure 1a), the optimal treatment rule based on the final outcome is more aligned with the optimal treatment rule defined in terms of later versus earlier surrogates. This implies that, despite requiring some time to measure and thus delaying adaptation in randomization probabilities, later surrogates are more useful in guiding treatment assignment probabilities. In Scenario 2 (Figure 1b), all surrogate outcomes have the same optimal treatment rule as that of the final outcome. Notably, early surrogates demonstrate a larger absolute value in the conditional average treatment effect (CATE) compared to later surrogates. This suggests that early surrogates are more sensitive to different treatments, potentially making them superior indicators of the most beneficial treatment compared to the final outcome. In other words, in this scenario, earlier surrogates have the joint advantage of both timeliness and improved

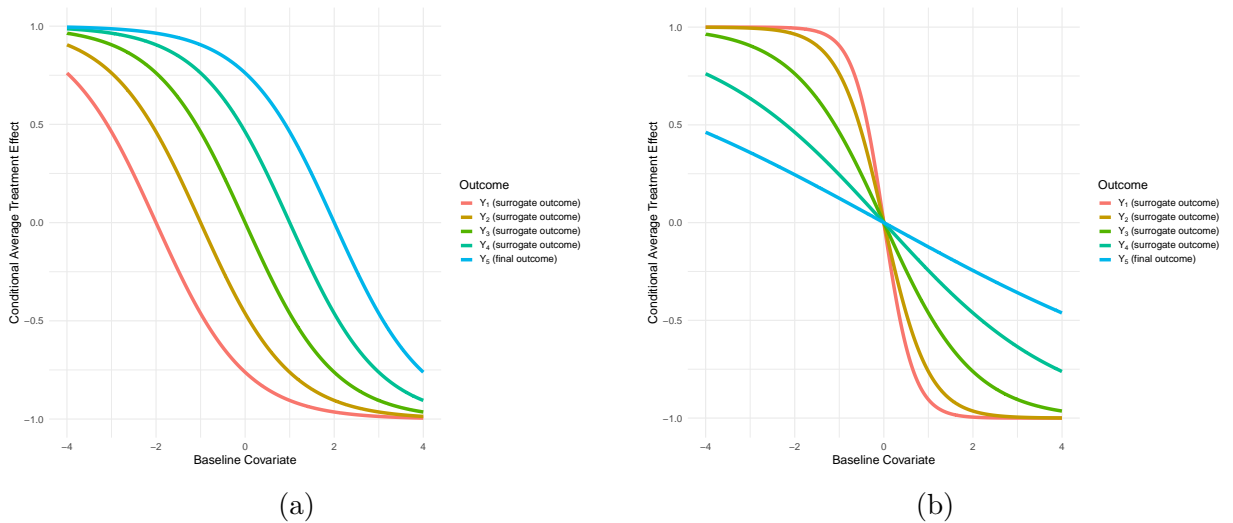


Figure 1: Conditional Average Treatment Effect (CATE) functions for the simulation scenarios: (a) Scenario 1, where later surrogates have higher utility; (b) Scenario 2, where earlier surrogates have higher utility. Each curve depicts the CATE function for a candidate outcome, Y_1 through Y_5 .

sensitivity for detecting treatment effect heterogeneity.

We compare seven distinct designs with varying treatment randomization mechanisms over 500 Monte Carlo runs: (a) a simple non-adaptive randomized controlled trial (RCT) design, which allocates two treatments with equal probability at each time point; (b) five adaptive designs with randomization probabilities updated in response to an *a priori* fixed choice of either a surrogate outcome Y_k ($k = 1, \dots, 4$) or the final outcome Y_K ($K = 5$); (c) the proposed TMLE-OSLAD adaptive design that dynamically evaluates and selects which outcome (among Y_1, \dots, Y_5) is used to update treatment randomization probabilities at each time point. For each design, we run experiments for $T = 50$ time points, enrolling 50 subjects at every time point, with the maximal probability of assigning the superior treatment capped at 90%.

Surrogate evaluation and TMLE performance. We first evaluate if TMLE-OSLAD can consistently identify the oracle surrogate, which we define as the candidate with the highest true $\Psi_{t,k}$ at time t among all Y_k (in other words, the surrogate that if used would result in

the largest expected primary outcomes for all enrolled participants in the experiment). In particular, if $\Psi_{t,K}$ is the largest, then the primary outcome Y_K itself is the oracle. Table 1 presents the average of true $\Psi_{t,k}$ values at illustrative time points 11, 21, 31, 41, and 50 for both scenarios across Monte Carlo runs. The expected outcome of Y_5 under the non-adaptive randomization is also reported, denoted by $\Psi_{t,RCT}$. In Scenario 1, the oracle surrogate gradually shifts towards later surrogates as time elapses and more data from these surrogates become available to guide the adaptation of treatment randomization probabilities. Initially, surrogates Y_3 and Y_4 have the highest value at times 11 and 21, reflecting the balance they achieve between earlier availability and degree to which they reflect the true optimal individualized treatment assignment. While these surrogates provide benefit in the short term, they do not consistently predict the correct optimal treatment for the primary outcome for all individuals, leading them to be eventually outperformed by designs that utilize the true primary outcome Y_5 as additional follow-up time is accrued. This is expected, as the ultimate assessment of a surrogate’s effectiveness as follow-up time extends hinges on its ability to predict the optimal personalized treatment for the primary outcome. In Scenario 2, as expected, surrogate Y_1 remains the most useful (i.e. is the oracle surrogate) throughout, due to its early availability, and the fact that it correctly identifies the true optimal individualized treatment for the long-term primary outcome. In contrast, later surrogates Y_4 and Y_5 have lower scores. This disparity can be attributed to the fact that while Y_4 and Y_5 will eventually serve equally well to identify the optimal personalized treatment as time since trial initiation goes to infinity, their utility is limited under finite trial durations because they have been observed for fewer participants. Across both scenarios, the TMLE estimates for these estimands exhibit low bias and variance, and their confidence intervals obtain nominal coverage (see Tables S1, S2, S3 in Appendix G). Figure 2 further tracks the frequency with which each candidate adaptive design is selected

Table 1: True target estimand $\Psi_{t,k}$ had participants enrolled from $1, \dots, t - K$ were adaptively treated by a candidate surrogate Y_k in Scenarios 1 and 2 ($t = 11, 21, 31, 41, 50$). Expected outcomes under oracle surrogate are shown in bold.

(a) Scenario 1							(b) Scenario 2						
t	$\Psi_{t,RCT}$	$\Psi_{t,1}$	$\Psi_{t,2}$	$\Psi_{t,3}$	$\Psi_{t,4}$	$\Psi_{t,5}$	t	$\Psi_{t,RCT}$	$\Psi_{t,1}$	$\Psi_{t,2}$	$\Psi_{t,3}$	$\Psi_{t,4}$	$\Psi_{t,5}$
11	0.000	-0.010	0.052	0.077	0.065	0.033	11	0.000	0.073	0.057	0.039	0.018	0.004
21	0.000	-0.006	0.082	0.144	0.174	0.170	21	0.000	0.086	0.080	0.072	0.059	0.037
31	0.000	-0.003	0.089	0.160	0.201	0.206	31	0.000	0.089	0.085	0.081	0.071	0.051
41	0.000	-0.001	0.092	0.168	0.214	0.223	41	0.000	0.091	0.088	0.084	0.076	0.058
50	0.000	0.001	0.094	0.172	0.221	0.233	50	0.000	0.092	0.090	0.086	0.080	0.063

by the proposed TMLE-OSLAD design at each time point t . Without prior knowledge of the relationships between surrogate and primary outcomes, the TMLE-OSLAD procedure is able to identify the oracle surrogate outcome in each setting. In Scenario 1, where later surrogate outcomes serve as better proxies for the final outcome when determining optimal individualized treatments, TMLE-OSLAD progressively shifts its selections toward these later surrogates, ultimately favoring Y_4 and Y_5 most frequently (see the left panel of Figure 2). In contrast, in Scenario 2 where the earliest surrogate Y_1 remains the oracle surrogate throughout, TMLE-OSLAD predominantly selects early surrogates, with Y_1 most frequently selected, followed by Y_2 and Y_3 , while Y_4 and Y_5 are rarely chosen.

Performance of benefiting participants. We use $d_{0,K} : \mathcal{W} \rightarrow \mathcal{A}$ to denote the true optimal individualized treatment rule for Y_K , which is defined as $d_{0,K}(W) := I(\bar{Q}_{0,K}(1, W) - \bar{Q}_{0,K}(0, W) > 0)$. This rule assigns to each individual the treatment that would maximize their expected final outcome, given their covariates. To evaluate the extent to which each design assigns treatments that match the underlying oracle optimal rule, we define probability (%) of not assigning optimal individualized treatments as $p_t^{non-opt} := \frac{1}{E(t)} \sum_{i:t_i=t} I(A_i \neq d_{0,K}(W_i))$, where $E(t)$ is the number of participants enrolled at time t . Similarly, $p_{t,RCT}^{non-opt}$ and $p_{t,SL}^{non-opt}$ denote this probability for the non-adaptive RCT and the proposed TMLE-OSLAD adaptive design, respectively. Table S4 in Appendix G compares these suboptimal treatment assignment probabilities across different designs. We also

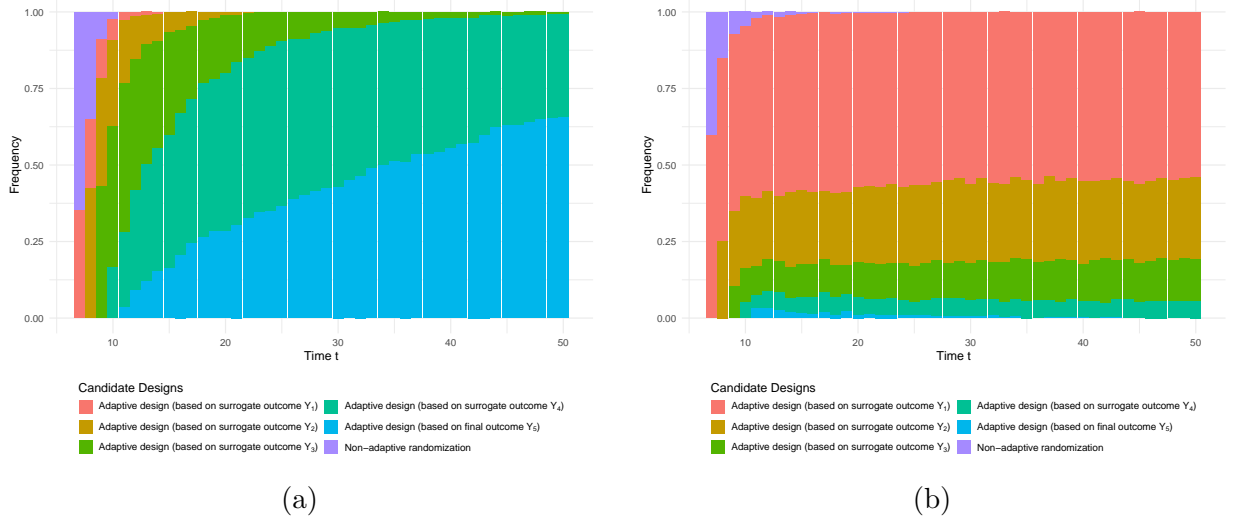


Figure 2: Frequency of candidate adaptive design selection by the Online Superlearner at each time point, differentiated by outcomes Y_k ($k \in \{1, 2, 3, 4, 5\}$). Panels (a) and (b) correspond to Scenario 1 and Scenario 2, respectively. Each color presents a candidate surrogate outcome / final outcome from Y_1 to Y_5 . The height of each bar indicates the frequency with which $\hat{\psi}_{t,k}$ has the highest lower bound of the confidence interval relative to the other $\hat{\psi}_{t,k'} (k' \neq k)$.

define the average regret for participants enrolled at time t within an adaptive design as $R_t := \frac{1}{E(t)} \sum_{i:t_i=t} I(A_i \neq d_{0,K}(W_i)) \times |\bar{Q}_{0,K}(1, W) - \bar{Q}_{0,K}(0, W)|$. Here, each participant i contributes the absolute difference in expected final outcomes between the optimal and actual treatments. A lower R_t indicates a better design that brings benefit in Y_K for participants enrolled at time t . We use $R_{t,k}$ to denote the average regret within an adaptive design responsive to Y_k at time t , while $R_{t,RCT}$ and $R_{t,SL}$ represent the average regret for the RCT design and TMLE-OSLAD design, respectively. Table S5 reports the average regret of these designs across 500 Monte Carlo simulations at times $t = 11, 21, 31, 41$, and 50. The regret trajectories for different designs are shown as line plots in Figure S1.

In Scenario 1, where later surrogates are superior at identifying the optimal individualized treatment, the adaptive design responsive to Y_5 , as expected, consistently demonstrates the lowest regret across the experiment. In contrast, in Scenario 2, the regret within the adaptive design that responds to Y_1 remains consistently the lowest. There is a noticeable trend that

the adaptive design in response to the final outcome Y_5 exhibits a slower convergence toward the regret of the oracle surrogate Y_1 , with a substantial discrepancy in regret that persists even at $t = 50$. Of course, in practice, the oracle surrogate is not known *a priori*, motivating the use of the TMLE-OSLAD procedure to evaluate and select among candidate surrogates in adaptive design. Across both scenarios, the proposed adaptive design demonstrates stable efficacy in approximating the minimal achievable regret compared to other designs. Its regret ranks second lowest starting at $t = 23$ in Scenario 1, and matches the lowest regret trajectory of Y_1 following $t = 21$ in Scenario 2. This robust performance reflects the advantage of the real-time evaluation and selection mechanism in TMLE-OSLAD, which continuously assesses each candidate surrogate-guided adaptive design, selects the most advantageous one to guide treatment randomization in subsequent stages.

Post-experiment inference for other causal estimands. Table 2 reports TMLE performance in estimating the additional causal estimands introduced in Section 3.3, including the average treatment effect and the mean final outcome under the estimated optimal treatment rules. The mean final outcome Y_5 under the estimated optimal treatment rule for Y_5 is estimated by two-fold CV-TMLE. Across all estimands, TMLE provides robust performance with low bias and variance, and nominal coverage of its confidence intervals.

6 Application

We conduct an extended simulation study inspired by the Adaptive Strategies for Preventing and Treating Lapses of Retention in HIV Care (ADAPT-R) trial (Geng et al., 2023), a sequential multiple assignment randomized (SMART) trial designed to evaluate adaptive strategies for improving retention in care among individuals initiating HIV treatment. We demonstrate our proposed TMLE-OSLAD framework in this context, showing how it utilizes effective surrogates to benefit participants and evaluating TMLE performance in this setup.

Table 2: Performance of TMLE estimators for other causal estimands at the end of experiments in Scenarios 1 and 2.

(a) Scenario 1						
Estimand	Notation	Truth	Bias ($\times 10^{-3}$)	Var ($\times 10^{-3}$)	Coverage (%)	
Average Treatment Effect on Final Outcome Y_5	$\psi_{n,5,T_{end}}^{ATE}$	0.470	1.60	3.83	95.2	
Expected Final Outcome Y_5 under OTR of Surrogate Y_1	$\psi_{d_{n,1,T_{end}}}^*$	0.015	0.92	2.28	95.2	
Expected Final Outcome Y_5 under OTR of Surrogate Y_2	$\psi_{d_{n,2,T_{end}}}^*$	0.130	0.55	1.85	94.8	
Expected Final Outcome Y_5 under OTR of Surrogate Y_3	$\psi_{d_{n,3,T_{end}}}^*$	0.237	-0.97	1.50	95.4	
Expected Final Outcome Y_5 under OTR of Surrogate Y_4	$\psi_{d_{n,4,T_{end}}}^*$	0.313	-0.89	0.97	95.0	
Expected Final Outcome Y_5 under OTR of Y_5	$\psi_{d_{n,5,T_{end}}}^*$	0.338	-2.00	0.87	94.6	

(b) Scenario 2						
Estimand	Notation	Truth	Bias ($\times 10^{-3}$)	Var ($\times 10^{-3}$)	Coverage (%)	
Average Treatment Effect on Final Outcome Y_5	$\psi_{n,5,T_{end}}^{ATE}$	0.062	0.04	3.89	95.4	
Expected Final Outcome Y_5 under OTR of Surrogate Y_1	$\psi_{d_{n,1,T_{end}}}^*$	0.120	1.04	0.49	95.2	
Expected Final Outcome Y_5 under OTR of Surrogate Y_2	$\psi_{d_{n,2,T_{end}}}^*$	0.120	1.12	0.50	94.8	
Expected Final Outcome Y_5 under OTR of Surrogate Y_3	$\psi_{d_{n,3,T_{end}}}^*$	0.120	0.90	0.51	95.4	
Expected Final Outcome Y_5 under OTR of Surrogate Y_4	$\psi_{d_{n,4,T_{end}}}^*$	0.119	0.77	0.51	95.0	
Expected Final Outcome Y_5 under OTR of Y_5	$\psi_{d_{n,5,T_{end}}}^*$	0.106	1.58	1.32	93.0	

Simulation setup. We focus on Phase 2 of the ADAPT-R trial, where participants who had a lapse in care in Phase 1 (defined as missing a clinic visit by 14 or more days) were re-randomized to a re-engagement strategy: either a peer navigation strategy (Navigator) or a combined Short Message Service reminder of appointments and conditional cash transfer (SMS+CCT). We discretize the study timeline into 50-day stages and define outcomes as the proportion of time in care during which a participant is engaged in across five windows, from the first day of receiving the re-engagement strategy to five specific time points: 50, 100, 150, 200, and 250 days. These outcomes are labeled as Y_1 , Y_2 , Y_3 , Y_4 , and Y_5 , respectively, with Y_5 (proportion of time in care in 250 days) the primary outcome, and Y_1 through Y_4 the surrogate outcomes. We consider two covariates in the conditioning set of heterogeneous treatment effect: (a) initial Phase 1 treatment arm: SMS, CCT, or standard of care (SOC) and (b) time from Phase 1 enrollment to initial lapse in care. We used data from 215 participants who were assigned either Navigator or SMS+CCT in Phase 2 after a lapse in care in Phase 1 and fit a generalized linear model to obtain the counterfactual outcomes for simulation. The CATE functions for the surrogate outcomes and the final outcome are presented in Figure S10 (see Appendix I with more details). We implement a series of CARA

designs as outlined in Section 5, including a simple sequential RCT, five adaptive designs that use a fixed choice from Y_1 through Y_5 , and the proposed TMLE-OSLAD adaptive design that evaluates and selects the best surrogate in real time. We also compared their performance with a naive policy that employs the latest available outcome at each time point to adapt treatment randomization probabilities. In each simulation, participants arrive following the enrollment schedule in the original trial with their observed covariates, and treatment assignments are generated sequentially according to the type of the simulated design and the covariate, treatment and outcome data of previously enrolled participants, then the outcomes are generated in response to the assigned treatment. This construction ensures that each observation is conditionally independent given the past. We simulate each design 500 times to assess the performance of TMLEs and different adaptive designs.

Results. We compare regret over time obtained from implementing different design strategies (Figure S11 in Appendix I). The adaptive design using the earliest outcome Y_1 outperforms those based on later outcomes or the naive policy from $t = 2$ through $t = 11$. After $t = 12$, adaptive designs using later outcomes start achieving smaller regret for new subjects than the earliest ones, as the underlying true CATE functions of later surrogates are closer to that for the final outcome and are estimated more precisely as data accumulate. However, this modest and delayed improvement does not compensate the overarching benefit provided by the earliest surrogate, which deliver prompt benefits to participants by adopting surrogate-guided optimal personalized treatments learned from more sufficient data. For the naive policy, although it initially matches the best performing adaptive design based on Y_1 , its aggressive shift to the most recent outcomes leads it to behave similarly to the suboptimal later-outcome designs, resulting in higher regret. In contrast, as shown in Figure 3a, TMLE-OSLAD predominantly selects the earliest surrogates (Y_1 and Y_2) over time. This makes the proposed adaptive design yields higher expected final outcome (Figure 3b) than

designs that adhere to later outcomes without ongoing evaluation, and comes close to the performance of the oracle design that uses the earliest surrogate. TMLE performance in estimating the proposed estimands within experiment and other estimands at the end of the experiment are reported in Appendix I, all demonstrating its robust estimation capability.

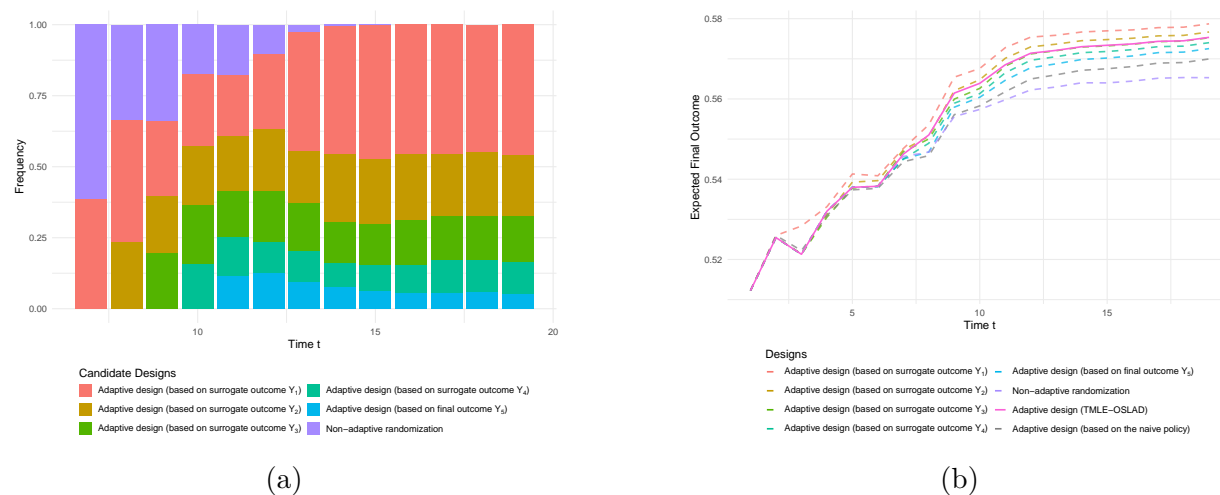


Figure 3: Panel (a) shows the frequency of candidate adaptive design selections by TMLE-OSLAD at each time point in the ADAPT-R trial simulation. Panel (b) shows the cumulative expected final outcome over time obtained from implementing different designs.

7 Conclusions

In summary, this work provides a general TMLE-based Online-Superlearner Adaptive-Design Framework (TMLE-OSLAD) for constructing a real-time, data-driven ensemble system for adaptive experimental designs and shows how this framework contributes to the statistical theory and application of surrogate outcomes in adaptive designs. We propose a novel causal estimand for surrogate utility in sequential adaptive designs: the mean primary outcome under a counterfactual CARA design where, at enrollment, each participant’s randomization is shifted toward the optimal individualized rule learned from a candidate surrogate. It captures both how well the surrogate guides optimal treatment assignment and the extent to which they enable earlier benefit for more participants, with

the goal of improving participants’ primary outcomes. Building on this, we define an Online-Superlearner adaptive design that incorporates the proposed estimand to evaluate a library of candidate surrogates, selects the most useful surrogate based on TMLE inference, and dynamically adapts randomization probabilities by the selected surrogate-guided design.

This work on surrogate outcomes is a concrete application of our highly general TMLE-OSLAD framework, which provides statistical inference on the mean counterfactual outcome under each candidate adaptive design in a user-supplied set, and adaptively evaluates and updates the best-performing design over time to adapt treatment randomization for new participants. This unified framework enables principled evaluation of the opportunities and costs of diverse adaptive designs varying in different design choices, quantifies how accumulating information benefits participants over time, and supports dynamic navigation of trade-offs among multiple designs during an ongoing experiment.

Methodologically, this framework advances non-parametric statistical inference for adaptive experiments: the proposed TMLE approach yields consistent, asymptotically normal estimators for the proposed estimand and other classical causal estimands, leveraging martingale theories, equicontinuity results, and Highly Adaptive Lasso. It broadly applies to estimation of various estimands in sequentially dependent settings like adaptive designs and time series.

Beyond the proposed context-specific estimand, further study of the computationally intensive “ideal estimand”, the expected outcome under the full data distribution induced by a candidate design (as discussed in Appendix A.2), could provide more insight into the strengths and limitations of different estimands, as well as the trade-offs between statistical properties and computational efficiency. We leave this to future work.

References

- Atkinson, A. C., Biswas, A., and Pronzato, L. (2011). Covariate-balanced response-adaptive designs for clinical trials with continuous responses that target allocation probabilities. Technical Report NI11042-DAE, Isaac Newton Institute for Mathematical Sciences, Cambridge, UK.
- Benkeser, D. and van der Laan, M. (2016). The highly adaptive lasso estimator. In *2016 IEEE International Conference on Data Science and Advanced Analytics (DSAA)*, pages 689–696.
- Bibaut, A., Dimakopoulou, M., Kallus, N., Chambaz, A., and van der Laan, M. (2021). Post-contextual-bandit inference. *Advances in Neural Information Processing Systems*, 34:28548–28559.
- Bibaut, A. F. and van der Laan, M. J. (2019). Fast rates for empirical risk minimization over càdlàg functions with bounded sectional variation norm. *arXiv preprint arXiv:1907.09244*.
- Breiman, L. (2001). Random forests. *Machine Learning*, 45:5–32.
- Brown, B. M. (1971). Martingale central limit theorems. *The Annals of Mathematical Statistics*, 42:59–66.
- Bubeck, S., Cesa-Bianchi, N., et al. (2012). Regret analysis of stochastic and nonstochastic multi-armed bandit problems. *Foundations and Trends in Machine Learning*, 5(1):1–122.
- Buyse, M., Molenberghs, G., Burzykowski, T., Renard, D., and Geys, H. (2000). The validation of surrogate endpoints in meta-analyses of randomized experiments. *Biostatistics*, 1(1):49–67.
- Chambaz, A. and van der Laan, M. J. (2011). Targeting the optimal design in randomized clinical trials with binary outcomes and no covariate: simulation study. *The International Journal of Biostatistics*, 7(1).
- Chambaz, A. and van der Laan, M. J. (2014). Inference in targeted group-sequential covariate-adjusted randomized clinical trials. *Scandinavian Journal of Statistics*, 41(1):104–140.

- Chambaz, A., Zheng, W., and van der Laan, M. J. (2017). Targeted sequential design for targeted learning inference of the optimal treatment rule and its mean reward. *The Annals of Statistics*, 45(6):2537–2564.
- Chen, T. and Guestrin, C. (2016). Xgboost: A scalable tree boosting system. In *Proceedings of the 22nd ACM SIGKDD International Conference on Knowledge Discovery and Data Mining*, KDD '16, pages 785–794. Association for Computing Machinery.
- Cheung, S. H., Zhang, L.-X., Hu, F., and Chan, W. S. (2014). Covariate-adjusted response-adaptive designs for generalized linear models. *Journal of Statistical Planning and Inference*, 149:152–161.
- Chow, S.-C. and Chang, M. (2008). Adaptive design methods in clinical trials—a review. *Orphanet Journal of Rare Diseases*, 3(1):11.
- Daniels, M. J. and Hughes, M. D. (1997). Meta-analysis for the evaluation of potential surrogate markers. *Statistics in Medicine*, 16(17):1965–1982.
- Duan, W., Ba, S., and Zhang, C. (2021). Online experimentation with surrogate metrics: Guidelines and a case study. In *Proceedings of the 14th ACM International Conference on Web Search and Data Mining*, pages 193–201.
- Elliott, M. R. (2023). Surrogate endpoints in clinical trials. *Annual Review of Statistics and its Application*, 10:75–96.
- Freedman, L. S., Graubard, B. I., and Schatzkin, A. (1992). Statistical validation of intermediate endpoints for chronic diseases. *Statistics in Medicine*, 11(2):167–178.
- Gao, J., Hu, F., and Ma, W. (2024). Response-adaptive randomization procedure in clinical trials with surrogate endpoints. *Statistics in Medicine*, 43(30):5911–5921.
- Geng, E. H., Odeny, T. A., Montoya, L. M., Iguna, S., Kulzer, J. L., Adhiambo, H. F., Eshun-Wilson, I., Akama, E., Nyandieka, E., Guzé, M. A., Shade, S., Packel, L., Fox, B., Camlin, C., Thirumurthy, H., Lyons, C., Bukusi, E. A., and Petersen, M. L. (2023). Adaptive strategies for retention in care among persons living with hiv. *NEJM Evidence*, 2(4):EVIDoA2200076.

- Gilbert, P. B. and Hudgens, M. G. (2008). Evaluating candidate principal surrogate endpoints. *Biometrics*, 64(4):1146–1154.
- Gill, R. D., van der Laan, M. J., and Wellner, J. A. (1995). Inefficient estimators of the bivariate survival function for three models. *Annales de l'Institut Henri Poincaré, Probabilités et Statistiques*, 31(3):545–597.
- Hadad, V., Hirshberg, D. A., Zhan, R., Wager, S., and Athey, S. (2021). Confidence intervals for policy evaluation in adaptive experiments. *Proceedings of the National Academy of Sciences*, 118(15):e2014602118.
- Hsu, J. Y., Kennedy, E. H., Roy, J. A., Stephens-Shields, A. J., Small, D. S., and Joffe, M. M. (2015). Surrogate markers for time-varying treatments and outcomes. *Clinical Trials*, 12(4):309–316.
- Hu, F. and Rosenberger, W. F. (2006). *The Theory of Response-Adaptive Randomization in Clinical Trials*. John Wiley & Sons.
- Hu, J., Zhu, H., and Hu, F. (2015). A unified family of covariate-adjusted response-adaptive designs based on efficiency and ethics. *Journal of the American Statistical Association*, 110(509):357–367.
- Huang, X., Ning, J., Li, Y., Estey, E., Issa, J.-P., and Berry, D. A. (2009). Using short-term response information to facilitate adaptive randomization for survival clinical trials. *Statistics in Medicine*, 28(12):1680–1689.
- Larsen, N., Stallrich, J., Sengupta, S., Deng, A., Kohavi, R., and Stevens, N. T. (2024). Statistical challenges in online controlled experiments: A review of a/b testing methodology. *The American Statistician*, 78(2):135–149.
- Lattimore, T. and Szepesvári, C. (2020). *Bandit Algorithms*. Cambridge University Press.
- Lin, D., Fleming, T., and De Gruttola, V. (1997). Estimating the proportion of treatment effect explained by a surrogate marker. *Statistics in Medicine*, 16(13):1515–1527.

- Luedtke, A. R. and van der Laan, M. J. (2016a). Statistical inference for the mean outcome under a possibly non-unique optimal treatment strategy. *The Annals of Statistics*, 44(2):713–742.
- Luedtke, A. R. and van der Laan, M. J. (2016b). Super-learning of an optimal dynamic treatment rule. *The International Journal of Biostatistics*, 12(1):305–332.
- Malenica, I., Bibaut, A., and van der Laan, M. J. (2021). Adaptive sequential design for a single time-series. *arXiv preprint arXiv:2102.00102*.
- Malenica, I., Coyle, J. R., van der Laan, M. J., and Petersen, M. L. (2024). Adaptive sequential surveillance with network and temporal dependence. *Biometrics*, 80(1):ujad007.
- McDonald, T. M., Maystre, L., Lalmas, M., Russo, D., and Ciosek, K. (2023). Impatient bandits: Optimizing recommendations for the long-term without delay. In *Proceedings of the 29th ACM SIGKDD Conference on Knowledge Discovery and Data Mining*, pages 1687–1697.
- Montoya, L. M., van der Laan, M. J., Luedtke, A. R., Skeem, J. L., Coyle, J. R., and Petersen, M. L. (2021). The optimal dynamic treatment rule superlearner: considerations, performance, and application to criminal justice interventions. *The International Journal of Biostatistics*, 19(1):217–238.
- Murphy, S. A. (2003). Optimal dynamic treatment regimes. *Journal of the Royal Statistical Society Series B: Statistical Methodology*, 65(2):331–355.
- Nowacki, A. S., Zhao, W., and Palesch, Y. Y. (2017). A surrogate-primary replacement algorithm for response-adaptive randomization in stroke clinical trials. *Statistical Methods in Medical Research*, 26(3):1078–1092.
- Pearl, J. (2000). *Causality: Models, Reasoning, and Inference*. Cambridge University Press.
- Prentice, R. L. (1989). Surrogate endpoints in clinical trials: definition and operational criteria. *Statistics in Medicine*, 8(4):431–440.

- Richardson, L., Zito, A., Greaves, D., and Soriano, J. (2023). Pareto optimal proxy metrics. *arXiv preprint arXiv:2307.01000*.
- Robbins, H. (1952). Some aspects of the sequential design of experiments. *Bulletin of the American Mathematical Society*, 58(5):527–535.
- Robertson, D. S., Lee, K. M., López-Kolkovska, B. C., and Villar, S. S. (2023). Response-adaptive randomization in clinical trials: From myths to practical considerations. *Statistical Science*, 38(2):185–208.
- Robins, J. M. (2004). Optimal structural nested models for optimal sequential decisions. In *Proceedings of the Second Seattle Symposium in Biostatistics*, pages 189–326. Springer.
- Robins, J. M. and Greenland, S. (1992). Identifiability and exchangeability for direct and indirect effects. *Epidemiology*, 3(2):143–155.
- Rosenberger, W. F. and Sverdlov, O. (2008). Handling covariates in the design of clinical trials. *Statistical Science*, 23(3):404–419.
- Rosenberger, W. F., Vidyashankar, A., and Agarwal, D. K. (2001). Covariate-adjusted response-adaptive designs for binary response. *Journal of Biopharmaceutical Statistics*, 11(4):227–236.
- Simchi-Levi, D. and Wang, C. (2023). Multi-armed bandit experimental design: Online decision-making and adaptive inference. In *International Conference on Artificial Intelligence and Statistics*, pages 3086–3097. PMLR.
- Tamura, R. N., Faries, D. E., Andersen, J. S., and Heiligenstein, J. H. (1994). A case study of an adaptive clinical trial in the treatment of out-patients with depressive disorder. *Journal of the American Statistical Association*, 89(427):768–776.
- Thompson, W. R. (1933). On the likelihood that one unknown probability exceeds another in view of the evidence of two samples. *Biometrika*, 25(3-4):285–294.
- van de Geer, S. A. (2000). *Empirical Processes in M-Estimation*. Cambridge University Press.

- van der Laan, M. J. (2006). Statistical inference for variable importance. *The International Journal of Biostatistics*, 2(1).
- van der Laan, M. J. (2008). The construction and analysis of adaptive group sequential designs. *U.C. Berkeley Division of Biostatistics*. Working Paper 232. <https://biostats.bepress.com/ucbbiostat/paper232>.
- van der Laan, M. J. (2015). A generally efficient targeted minimum loss based estimator. *U.C. Berkeley Division of Biostatistics*. Working Paper 343. <https://biostats.bepress.com/ucbbiostat/paper343>.
- van der Laan, M. J. (2023). Higher order spline highly adaptive lasso estimators of functional parameters: Pointwise asymptotic normality and uniform convergence rates. *arXiv preprint arXiv:2301.13354*.
- van der Laan, M. J. and Luedtke, A. R. (2015). Targeted learning of the mean outcome under an optimal dynamic treatment rule. *Journal of Causal Inference*, 3(1):61–95.
- van der Laan, M. J. and Malenica, I. (2018). Robust estimation of data-dependent causal effects based on observing a single time-series. *arXiv preprint arXiv:1809.00734*.
- van der Laan, M. J., Polley, E. C., and Hubbard, A. E. (2007). Super learner. *Statistical Applications in Genetics and Molecular Biology*, 6(1).
- van der Laan, M. J. and Rose, S. (2011). *Targeted Learning: Causal Inference for Observational and Experimental Data*. Springer.
- van der Laan, M. J. and Rose, S. (2018). *Targeted Learning in Data Science*. Springer.
- van der Laan, M. J. and Rubin, D. (2006). Targeted maximum likelihood learning. *The International Journal of Biostatistics*, 2(1).
- van Handel, R. (2011). On the minimal penalty for markov order estimation. *Probability Theory and Related Fields*, 150:709–738.

- VanderWeele, T. J. (2013). Surrogate measures and consistent surrogates. *Biometrics*, 69(3):561–565.
- Weir, C. J. and Taylor, R. S. (2022). Informed decision-making: Statistical methodology for surrogacy evaluation and its role in licensing and reimbursement assessments. *Pharmaceutical Statistics*, 21(4):740–756.
- Yang, J., Eckles, D., Dhillon, P., and Aral, S. (2024). Targeting for long-term outcomes. *Management Science*, 70(6):3841–3855.
- Zhan, R., Hadad, V., Hirshberg, D. A., and Athey, S. (2021). Off-policy evaluation via adaptive weighting with data from contextual bandits. In *Proceedings of the 27th ACM SIGKDD Conference on Knowledge Discovery & Data Mining*, pages 2125–2135.
- Zhang, L.-X., Hu, F., Cheung, S. H., and Chan, W. S. (2007). Asymptotic properties of covariate-adjusted response-adaptive designs. *The Annals of Statistics*, 35(3):1166–1182.
- Zhao, W., Ma, W., Wang, F., and Hu, F. (2022). Incorporating covariates information in adaptive clinical trials for precision medicine. *Pharmaceutical Statistics*, 21(1):176–195.
- Zheng, W. and van der Laan, M. J. (2011). *Cross-Validated Targeted Minimum-Loss-Based Estimation*, pages 459–474. Springer New York, New York, NY.
- Zhu, H. (2015). Covariate-adjusted response adaptive designs incorporating covariates with and without treatment interactions. *Canadian Journal of Statistics*, 43(4):534–553.

SUPPLEMENTARY MATERIAL of
“An Online Meta-Level Adaptive-Design Framework
with Targeted Learning Inference: Applications to
Evaluating and Utilizing Surrogate Outcomes in
Adaptive Designs”

A Additional Remarks on the Target Estimand

A.1 Surrogate Evaluation with Adaptive Design Perspective

Our approach adopts an adaptive-design perspective to evaluate surrogates in sequential decision-making contexts. The proposed target estimand evaluates the utility of surrogates by their early availability, predictability, and sensitivity in indicating effective treatments in the following sense. We define a trajectory of treatment rules $\tilde{g}_{k,1:t}^* := (\tilde{g}_{k,1}^*, \dots, \tilde{g}_{k,t}^*)$, with each rule $\tilde{g}_{k,t'}^*$ generating a personalized treatment randomization function $g_{k,i}^*$ for each participant i enrolled at time t' . Every $g_{k,i}^*$ is specifically tailored to maximize the surrogate outcome Y_k based on their baseline covariates W_i and context. We note that at each time point t' , $\tilde{g}_{k,t'}^*$ depends only on historical data $\bar{\mathcal{H}}(t')$. Therefore, $\tilde{g}_{k,t'}^*$ can not deviate from a static design with equal randomization probabilities during the initial k time points, as observation of Y_k is not yet available. Once Y_k is available at $t' = k + 1$, $\tilde{g}_{k,t'}^*$ starts moving towards its optimal treatment rule $d_{0,k}(W) := I(\bar{Q}_{0,k}(1, W) - \bar{Q}_{0,k}(0, W) > 0)$ over time. If $d_{0,k}$ closely aligns with the true optimal rule for the primary outcome $d_{0,K}$, then the surrogate Y_k demonstrates the advantage of its early availability in informing which treatment is better in the context of sequential decision making, compared to later outcomes. The progression of $\tilde{g}_{k,t'}^*$ from a static design with equal randomization probabilities towards the optimal treatment rule $d_{0,k}$ depends on the magnitude of treatment superiority (as measured

by the point estimate of CATE) and its uncertainty (as reflected by estimated standard error of CATE). Therefore, if a surrogate Y_k exhibits good alignment with the primary outcome in terms of optimal treatment rule and presents a strong signal of individualized optimal treatment over other surrogates, this surrogate will be preferred and given a higher $\Psi_{t,k}$. Of course, even if a surrogate demonstrates early availability and sensitivity, it will present a lower $\Psi_{t,k}$ value if it fails to predict optimal personalized treatments of the primary outcome. This is because the ultimate evaluation of a surrogate’s performance is based on the expected final outcome, underscoring the critical role of predictability in evaluating surrogate outcomes in adaptive designs.

In summary, our proposed target estimand provides a comprehensive measure of a candidate surrogate’s utility to accelerate participant benefit in sequential adaptive designs. It captures not only the timeliness with which the surrogate becomes available for early adaptation, but also its sensitivity to heterogeneous treatment effects and its predictive accuracy in identifying optimal personalized treatments for the primary outcome. This approach contrasts with existing surrogate evaluation methods, which are generally developed for static settings rather than from a dynamic adaptive design perspective.

A.2 Approximation of an Ideal Estimand

Ideally, one could fully evaluate a candidate adaptive design by defining an ideal estimand as the expected final outcome when the entire experiment is conducted under that design, averaged across all participants. Formally, this requires integrating over the joint distribution of entry-time histories, contexts, treatments, and outcomes that would be sequentially induced if the candidate adaptive design were implemented from the start of the experiment. In practice, however, targeting this estimand is computationally intensive and entails a substantially more involved estimation procedure.

Instead, our context-specific estimand provides a fast and robust approximation to the ideal estimand by evaluating the expected outcome under the candidate design using contexts of the observed histories under the actual experiment. This estimand avoids modeling the full induced distribution under the candidate design and admits doubly robust estimation via TMLE (see Section 4). The approximation is most accurate when the observed contexts from the actual experiment are representative of those the candidate design would induce - especially when the candidate design’s adaptation is based on learning from a stationary target such as Q_0 or CATE that dominates over the experiments. This provides an effective approach to distinguishing low-utility from high-utility adaptive designs, thereby facilitating online selection among candidate designs with robust statistical support.

In simulation studies, we also compute the expected counterfactual final outcome obtained by implementing each candidate adaptive design (see Table S7 in Appendix G), which corresponds to the ideal estimand. The results show that our context-specific estimand (Table 1) closely matches this ideal target with minimal differences.

B The Highly Adaptive Lasso Estimator

Highly Adaptive Lasso (HAL) (van der Laan, 2015; Benkeser and van der Laan, 2016) is a flexible non-parametric regression estimator that minimizes empirical risk over the class of càdlàg (right-continuous with left limits) functions with bounded sectional variation norms (Gill et al., 1995). Instead of relying on local smoothness assumptions, HAL imposes a global smoothness constraint through the sectional variation norm and achieves a convergence rate of order $n^{-1/3}$ up to logarithmic factors when using zero-order splines (Bibaut and van der Laan, 2019). Recent work by van der Laan (2023) studies higher-order smoothness classes of càdlàg functions and develops higher-order spline HAL, showing that the m -th order HAL is asymptotically normal and attains a uniform convergence rate of order $n^{-\frac{m+1}{2m+3}}$ up

to a logarithmic factor ($m = 1, 2, \dots$). In this work, we use first-order HAL to estimate conditional average treatment effect (CATE) functions (Appendix C) and provide a corollary for proving equicontinuity conditions of martingale processes based on theoretical results of higher-order spline HAL-MLEs, as shown in Appendices E and F.

We first introduce a class of d -variate càdlàg functions defined on a unit cube $[0, 1]^d$ with bounded sectional variation norm (Gill et al., 1995).

For any $x \in [0, 1]^d$, denote $x(j)$ as its j -th coordinate. For a given subset $s \subset \{1, \dots, d\}$, denote $x_s = (x(j) : j \in s)$. Let \bar{Q} be a real-valued d -variate càdlàg function on a unit cube $[0, 1]^d$. Define $\bar{Q}_s : (0_s, 1_s] \rightarrow \mathbb{R}$ as $\bar{Q}_s(u_s) = \bar{Q}(u_s, 0_{-s})$, i.e., the s -specific section of \bar{Q} that sets coordinates in the complement of subset s equal to 0. The sectional variation norm of \bar{Q} is defined by $\|\bar{Q}\|_v^* := |\bar{Q}(0)| + \sum_{s \subset \{1, \dots, d\}, s \neq \emptyset} \int_{(0_s, 1_s]} |d\bar{Q}(u_s, 0_{-s})|$. Suppose $\|\bar{Q}\|_v^*$ is finite, then \bar{Q} can be represented as (Gill et al., 1995):

$$\bar{Q}(x) = \int_{[0, x]} d\bar{Q}(u) = \bar{Q}(0) + \sum_{s \subset \{1, \dots, d\}, s \neq \emptyset} \int_{(0_s, 1_s]} \phi_{u_s}^{(0)}(x_s) d\bar{Q}(u_s, 0_{-s}),$$

where $\phi_{u_s}^{(0)}(x_s) := I(x_s \geq u_s)$ is a zero-order basis function.

One can use discrete measure with observed support points to approximate the presentation of \bar{Q} (van der Laan, 2015; Benkeser and van der Laan, 2016). Given n i.i.d samples (x_i, y_i) ($i = 1, \dots, n$) with $x_i \in [0, 1]^d$, $y_i \in \mathbb{R}$, one can use the s -specific support points $x_{s,i} := (x_i(j) : j \in s)$ observed for each unit i across different subsets s to approximate \bar{Q} . Specifically, the approximation is given by $\bar{Q}_\beta(x) = \beta_0 + \sum_{s \subset \{1, \dots, d\}} \sum_{i=1}^n \beta_{s,i} \phi_{x_{s,i}}^{(0)}(x(s))$.

We define $Pf := \int f(o) dP(o)$ for a function f with a data generating distribution P that generates data $O \sim P$. Let $P_n f := \int f(o) dP_n(o)$ under empirical distribution P_n . Define the class $\bar{\mathcal{Q}}_{n,C}^{(0)} = \left\{ \bar{Q}_\beta(x) : |\beta_0| + \sum_{s \subset \{1, \dots, d\}} \sum_{i=1}^n |\beta_{s,i}| < C \right\}$ for some constant C , and let $L(\bar{Q})$ be a loss function. A zero-order HAL-MLE is constructed by solving the following loss-based

minimization problem: $\bar{Q}_n = \operatorname{argmin}_{\bar{Q}_\beta \in \bar{\mathcal{Q}}_{n, C_n^u}^{(0)}} P_n L(\bar{Q}_\beta)$, where C_n^u is a data-adaptive cross-validation or undersmoothed selector of bounded sectional variation norm for the working model constructed on the basis functions $\phi_{x_{s,i}}^{(0)}$'s. [Bibaut and van der Laan \(2019\)](#) establishes the L_2 convergence rate of $n^{-\frac{1}{3}}$ up to logarithmic factors for the zero-order HAL-MLE.

[van der Laan \(2023\)](#) extends the HAL construction to higher-order smoothness classes. For integer $m \geq 1$, define the m -th order smoothness class $D^{(m)}([0, 1]^d)$ ($m = 1, 2, \dots$) on $[0, 1]^d$ as the class with functions whose m -th-order Lebesgue-Radon-Nikodym derivatives are càdlàg functions with bounded sectional variation norm. Like the zero-order HAL-MLE, one can construct a higher-order HAL-MLE that uses m -th order splines to estimate the target function in $D^{(m)}([0, 1]^d)$. For the first-order ($m = 1$), the approximation of $\bar{Q}^{(1)} \in D^{(1)}([0, 1]^d)$ can be written by $\bar{Q}_\beta^{(1)}(x) = \beta_0 + \sum_{s \subset \{1, \dots, d\}} \sum_{i=1}^n \beta_{s,i} \phi_{x_{s,i}}^{(1)}(x(s))$, where $\phi_u^{(1)}(x) = (x - u)I(x \geq u)$. Define $\bar{\mathcal{Q}}_{n, C}^{(1)} = \{\bar{Q}_\beta^{(1)} \in D^{(1)}([0, 1]^d) : |\beta_0| + \sum_{s \subset \{1, \dots, d\}} \sum_{i=1}^n |\beta_{s,i}| < C\}$. The first-order HAL-MLE is constructed by $\bar{Q}_n^{(1)} = \operatorname{argmin}_{\bar{Q}_\beta^{(1)} \in \bar{\mathcal{Q}}_{n, C_n^u}^{(1)}} P_n L(\bar{Q}_\beta^{(1)})$. One can also consider the second-order spline function $\phi_u^{(2)}(x) = \frac{1}{2}(x - u)^2 I(x \geq u)$ or higher-order spline basis functions to fit higher-order HAL-MLEs. Moreover, [van der Laan \(2023\)](#) establishes uniform covering number and entropy bounds for these higher-order HAL estimators, and shows that the m -th order spline HAL-MLE achieves asymptotic normality and a uniform convergence rate of $n^{-\frac{m+1}{2m+3}}$ up to logarithmic factors.

C Estimation of Conditional Average Treatment Effect

A key procedure in our adaptive design is estimating the conditional average treatment effect (CATE). By estimating the CATE function, the experimenter can identify the optimal treatment rule that maximizes the expected outcome conditional on baseline covariates, and update treatment randomization probabilities accordingly to increase the chance of allocating the estimated optimal personalized treatment in adaptive design.

In this work, we use the Highly Adaptive Lasso (HAL) estimator to estimate the CATE function, with its advantages introduced in Appendix B. Furthermore, we apply the delta-method to obtain a Wald-type confidence interval for the CATE. This confidence interval guides the exploration-exploitation trade-off in adaptive designs by adjusting treatment randomization probabilities based on the uncertainty in CATE estimates, which will be discussed in Appendix D.

Recall that $\bar{Q}_{0,k}(A, W) = E[Y_k|A, W]$ is the true conditional expectation of the k -th surrogate outcome, given the treatment A and baseline covariates W . For every new participant i enrolled at time t , we use $B_{n,k,t}(W_i)$ to denote an estimate of $B_{0,k}(W_i) := E[Y_k(1) - Y_k(0)|W_i]$, the true CATE of Y_k given W_i , the baseline covariates of participant i . We use $\tau_{n,k,t}(W_i)$ to denote the estimated standard error of CATE. Both estimates are based on $\mathcal{H}(i)$, the historical data observed before participant i is enrolled.

For each surrogate outcome Y_k , we estimate CATE functions by two steps. First, we transform Y_k into the pseudo-outcome (van der Laan, 2006; Luedtke and van der Laan, 2016b):

$$\eta_k(\bar{Q}_k, g)(O) = \frac{2A - 1}{g(A | W)} [Y_k - \bar{Q}_k(A, W)] + \bar{Q}_k(1, W) - \bar{Q}_k(0, W).$$

We note that the pseudo-outcome has the doubly-robust property that $E[\eta_k(\bar{Q}_k, g)(O) | W] = B_{0,k}(W)$ if $\bar{Q}_k = \bar{Q}_{0,k}$ or $g = g_0$. Since g_0 is known in adaptive design, we only need to estimate $\bar{Q}_{0,k}$ with $\bar{Q}_{n,k}$, then impute $\bar{Q}_{n,k,t}$ and g_0 to generate the pseudo-outcome $\eta_k(\bar{Q}_{n,k,t}, g_0)$.

Second, we estimate the CATE function $B_{0,k}$ by regressing the pseudo-outcome $\eta_k(\bar{Q}_{n,k,t}, g_0)$ on baseline covariates W by first-order spline HAL-MLE, which minimizes the empirical risk over $D^{(1)}([0, 1]^d)$, the first-order smoothness class with its first-order derivative being càdlàg function with bounded sectional variation norm. That is, at time t , we estimate the

CATE function by solving the following minimization problem:

$$B_{n,k,t} = \operatorname{argmin}_{B_k \in \bar{\mathcal{Q}}_{n,C_n^u}^{(1)}} P_n L_k(B_k).$$

where L_k is the loss function defined by $L_k(B_k)(O) := (B_k(W) - \eta_k(O))^2$; $n_{t,k} := N(t - k)$ is the number of participants with observed Y_k at time t ; C_n^u is an upper bound for the first-order sectional variation norm that is data-adaptively selected via cross-validation.

As introduced in Appendix B, $B_{n,k,t}(\cdot)$ can be written as a linear combination of first-order spline basis functions with non-zero coefficients. To quantify the uncertainty of the CATE, we use the delta method under this HAL working model to obtain pointwise inference for the conditional mean of the pseudo-outcome, which corresponds to the CATE. Let $\tau_{n,k,t}(W_i)$ denote the estimate of the standard error of $B_{n,k,t}(W_i)$; a Wald-type $100(1 - \alpha)\%$ confidence interval for the CATE at W_i is $B_{n,k,t}(W_i) \pm z_{1-\alpha/2} \tau_{n,k,t}(W_i)$. Both $B_{n,k,t}(W_i)$ and $\tau_{n,k,t}(W_i)$ are then incorporated into the treatment randomization function introduced in Appendix D to construct $g_{k,i}^*$ for each participant i in the adaptive design guided by surrogate Y_k .

D Details of CARA Procedures

We define a treatment randomization function $\tilde{h}_\nu : [-1, 1] \times \mathbb{R}^+ \rightarrow [0, 1]$ as follows:

$$\tilde{h}_\nu(x, b) = \nu I(x \leq -b) + (1 - \nu) I(x \geq b) + \left(-\frac{1/2 - \nu}{2b^3} x^3 + \frac{1/2 - \nu}{2b/3} x + \frac{1}{2} \right) I(-b < x < b),$$

where $\nu \in (0, 0.5)$ is a user-specified constant ensuring that $\nu \leq \tilde{h}_\nu \leq 1 - \nu$.

This mapping, adapted from (Chambaz et al., 2017), is extended here to explicitly incorporate both the magnitude and uncertainty of the estimated CATE. In our setup, x is the point estimate of CATE for each subject, while b is the estimated standard error of CATE, scaled

by the $z_{1-\alpha/2}$ quantile of the standard normal distribution.

For interpretability, it is helpful to re-express this function in terms of the standardized CATE $z = x/b$, which is the CATE divided by half the width of its confidence interval. The function then becomes

$$h_\nu(z) = \begin{cases} \nu, & z \leq -1 \\ \nu + (1 - 2\nu) \left(-\frac{1}{4}z^3 + \frac{3}{4}z + \frac{1}{2} \right), & -1 < z < 1 \\ 1 - \nu, & z \geq 1 \end{cases}$$

This function smoothly interpolates between balanced randomization and deterministic allocation of optimal personalized treatment based on the standardized CATE signal relative to uncertainty. When the signal is modest, a near-balanced allocation is maintained between treatment and control, avoiding over-commitment to a noisy or unstable estimated rule and ensuring continued learning of CATE by preserving exploration in both arms. As evidence accumulates and the magnitude of the CATE signal increases, the treatment randomization probability shifts further toward the estimated optimal treatment. Meanwhile, a minimal exploration probability is retained, which is necessary for estimating CATE during the experiment and a range of other causal estimands at the end of the adaptive experiment.

In our surrogate-guided adaptive designs, the treatment randomization probabilities are generated as follows. For each candidate surrogate outcome Y_k and each subject i with baseline covariates W_i , we estimate CATE $B_{n,k}(W_i)$ and its standard error $\tau_{n,k}(W_i)$ as detailed in Appendix C. Consequently, the treatment randomization probability for $a = 1$ is given by $h_\nu\left(\frac{B_{n,k}(W_i)}{z_{1-\alpha/2} \cdot \tau_{n,k}(W_i)}\right)$, and for $a = 0$ it is $1 - h_\nu\left(\frac{B_{n,k}(W_i)}{z_{1-\alpha/2} \cdot \tau_{n,k}(W_i)}\right)$, where $\nu = 0.1$. If the surrogate outcome Y_k has not yet been observed, the assignment defaults to equal randomization probability of 0.5.

E Equicontinuity Condition for a General Martingale Process

In this section, we provide a theorem about the equicontinuity condition of martingale processes in a general setup that includes but not limited to adaptive design settings.

E.1 Statistical Setup

Suppose we sequentially generate a sequence of data O_i from $i = 1$ to N . Every $O_i \in \mathcal{O}_i$ is generated from historical data $\bar{O}(i-1) := (O_1, \dots, O_{i-1})$. We define a probability triple $(\Omega, \mathcal{F}, \mathbf{P})$, where \mathcal{F}_i , ($i = 1, \dots, N, \dots$) are defined as sub-sigma-algebras $\mathcal{F}_1 \subset \dots \subset \mathcal{F}_N \subset \dots \subset \mathcal{F}$ with $\bar{O}(i) \in \mathcal{O}_1 \times \dots \times \mathcal{O}_i \subset \mathcal{F}_i$. We consider a scenario in which every O_i is generated based on $\bar{O}(i-1)$ through a fixed-dimensional summary measure $C_i \in \mathcal{C}$, where C_i is generated by a known function mapping from $\mathcal{O}_1 \times \dots \times \mathcal{O}_{i-1}$ to \mathcal{C} for every $i = 1, \dots, N$.

Let $f_\theta : \mathcal{O} \times \mathcal{C} \rightarrow \mathbb{R}$ be a \mathcal{F}_i -measurable function, indexed by a class of functions Θ . Define

$$M_N(\theta) = \frac{1}{N} \sum_{i=1}^N \left\{ f_\theta(O_i, C_i) - E \left[f_\theta(O_i, C_i) \mid \bar{O}(i-1) \right] \right\}.$$

Suppose there is an unknown element $\theta^* \in \Theta$ to be estimated by $\theta_N \in \Theta$ based on data $\bar{O}(N)$. We provide a general theorem for the equicontinuity condition with respect to the martingale process as follows:

$$M_{2,N}(\theta_N, \theta^*) := M_N(\theta_N) - M_N(\theta^*) = o_P(N^{-\frac{1}{2}}).$$

E.2 Proof of Equicontinuity Condition

We first restate a bracketing entropy based on Definition A.1 in [van Handel \(2011\)](#) (which was introduced by Definition 8.1 in [van de Geer \(2000\)](#)) in our notation.

Definition E.1. (*Bracketing entropy for martingales*) Consider a stochastic process of the form $\{(\xi_{\theta,i})_{i=1}^N : \theta \in \Theta\}$ where Θ is an index set such that, for every $\theta \in \Theta, i \in [N]$, $\xi_{\theta,i}$ is an $\bar{O}(i)$ -measurable random variable for all i and θ . Denote $F := \bar{O}(N) \in \mathcal{F}$. We say that a collection of random variables of the form $\mathcal{B} := \{(\Lambda_i^j, \Upsilon_i^j)_{i=1}^N : j \in [J]\}$ is an $(N, \Theta, F, Z, \epsilon)$ -bracketing if

1. for every $i \in [N]$, and $j \in [J]$, $(\Lambda_i^j, \Upsilon_i^j)$ is $\bar{O}(i)$ -measurable,
2. for every $\theta \in \Theta$, there exists $j \in [J]$, such that, for every $i \in [N]$, $\Lambda_i^j \leq \xi_{\theta,i} \leq \Upsilon_i^j$,
3. for every $j \in [J]$,

$$\frac{2Z^2}{N} \sum_{i=1}^N E \left[\phi \left(\frac{\Upsilon_i^j - \Lambda_i^j}{Z} \right) \mid \bar{O}(i-1) \right] \leq \epsilon^2,$$

where $\phi(x) = e^x - x - 1$. We denote $\mathcal{N}_{[]} (N, \Theta, F, Z, \epsilon)$ the minimal cardinality of an $(N, \Theta, \mathcal{F}, Z, \epsilon)$ -bracketing. We define the bracketing entropy integral as $\mathcal{J}_{[]} (N, \Theta, F, Z, \epsilon) := \int_0^\epsilon \mathcal{N}_{[]} (N, \Theta, F, Z, u) du$.

Theorem E.1 (Theorem A.4 in [van Handel \(2011\)](#)). Given $Z > 0$, for all $i \geq 0$, define

$$M_{\theta,i} = \frac{1}{N} \sum_{l=1}^i (\xi_{\theta,l} - E[\xi_{\theta,l} \mid \mathcal{F}_{l-1}]),$$

$$R_{\theta,i} = \frac{1}{N} 2Z^2 \sum_{l=1}^i E \left[\phi \left(\frac{|\xi_{\theta,l}|}{Z} \right) \mid \mathcal{F}_{l-1} \right].$$

By Theorem A.4 in [van Handel \(2011\)](#), for any $N \in \mathbb{N}$, $x > 0$, and $0 < R < \infty$,

$$P \left(\sup_{\theta \in \Theta} I(R_{\theta, N} \leq R) \max_{i \in [N]} \sqrt{N} M_{\theta, i} \geq 16\Gamma + 32\sqrt{Rx} + \frac{16}{\sqrt{N}} Zx \right) \leq 2e^{-x},$$

where $\Gamma := \frac{Z}{\sqrt{N}} \log \mathcal{N}_{[]} (N, \Theta, F, Z, \sqrt{R}) + 4\mathcal{J}_{[]} (N, \Theta, F, Z, \sqrt{R})$.

We focus on the process of $\xi_{\theta, i} = f_{\theta}(O_i, C_i) - f_{\theta^*}(O_i, C_i)$ ($i = 1, \dots, n$), with $\theta^* \in \Theta, \theta \in \Theta$.

As the bracketing entropy condition may be hard to check because of its intricate definition, we relate it to the supremum norm covering entropy, following the approach outlined by [van de Geer \(2000\)](#) in Section 8.2 and [Chambaz and van der Laan \(2011\)](#) in Lemma 7. Our method slightly differs from their approaches in that we relate the bracketing entropy to the supremum norm covering entropy for Θ instead of $\{f_{\theta} : \theta \in \Theta\}$.

Assumption E.1 (Entropy Integral). Let $\mathcal{N}_{\infty}(\epsilon, \Theta)$ denote the ϵ -covering number in supremum norm of Θ and let $\mathcal{J}_{\infty}(\epsilon, \Theta) := \int_0^{\epsilon} \sqrt{\log(1 + \mathcal{N}_{\infty}(u, \Theta))} du$ denote the ϵ -entropy integral in supremum norm of Θ . Assume that $\mathcal{J}_{\infty}(\epsilon, \Theta)$ is finite and $\mathcal{J}_{\infty}(\epsilon, \Theta) \rightarrow 0$ as $\epsilon \rightarrow 0$.

Assumption E.2 (Uniform Boundedness). $\sup_{\theta \in \Theta} \|\theta\|_{\infty} < \infty$, $\sup_{\theta \in \Theta} \|f_{\theta}\|_{\infty} < \infty$.

Assumption E.3. $\sup_{\theta_1 \in \Theta, \theta_2 \in \Theta, \theta_1 \neq \theta_2} \frac{\|f_{\theta_1} - f_{\theta_2}\|_{\infty}}{\|\theta_1 - \theta_2\|_{\infty}} < \infty$.

Lemma E.1. Suppose that Assumptions [E.1](#), [E.2](#) and [E.3](#) hold, such that $\|\theta\|_{\infty} < M$ for some finite constant $M > 0$ and $\sup_{\theta_1 \in \Theta, \theta_2 \in \Theta, \theta_1 \neq \theta_2} \frac{\|f_{\theta_1} - f_{\theta_2}\|_{\infty}}{\|\theta_1 - \theta_2\|_{\infty}} \leq L$ for some finite constant $L > 0$. Then the following holds:

$$\mathcal{N}_{[]} (N, \Theta, F, 8LM, 2\sqrt{2}L\epsilon) \leq \mathcal{N}_{\infty}(\epsilon, \Theta),$$

and

$$\mathcal{J}_{[]} (N, \Theta, F, 8LM, 2\sqrt{2}L\epsilon) \leq \mathcal{J}_{\infty}(\epsilon, \Theta).$$

Proof. Suppose $\{\theta_j : j \in [J]\} \subset \Theta$ is an ϵ -covering of Θ in supremum norm such that $\forall \theta \in \Theta$, there exists $j \in [J]$ such that $\theta_j \in \Theta$ and $\|\theta_j - \theta\|_\infty \leq \epsilon$. Denoting $\lambda_j = \theta_j - \epsilon$ and $v_j = \theta_j + \epsilon$. With Assumption E.2, we can let $\epsilon \leq 2M$ as $\lambda_j = \theta_j - M$ and $v_j = \theta_j + M$ always construct a valid pair of brackets. Under Assumption E.3, $\|f_{\theta_j} - f_\theta\|_\infty \leq L \|\theta_j - \theta\|_\infty \leq L\epsilon$. Define $\Lambda_i^j = f_{\theta_j} - L\epsilon$ and $\Upsilon_i^j = f_{\theta_j} + L\epsilon$. Then, we have that

$$\frac{1}{N} 2Z^2 \sum_{i=1}^N E \left[\phi \left(\frac{|\Upsilon_i^j - \Lambda_i^j|}{Z} \right) \mid \bar{O}(i-1) \right] \leq 2Z^2 \phi \left(\frac{2L\epsilon}{Z} \right) \leq 2Z^2 \sum_{p \geq 2} \frac{1}{p!} \frac{p!}{2} \left(\frac{2L\epsilon}{Z} \right)^p = \frac{2L\epsilon}{\frac{1}{2L\epsilon} - \frac{1}{Z}}.$$

Let $Z = 8LM$. We have that

$$\frac{1}{N} 2Z^2 \sum_{i=1}^N E \left[\phi \left(\frac{|\Upsilon_i^j - \Lambda_i^j|}{Z} \right) \mid \bar{O}(i-1) \right] \leq (2\sqrt{2}L\epsilon)^2.$$

Therefore,

$$\mathcal{N}_\square(N, \Theta, F, 8LM, 2\sqrt{2}L\epsilon) \leq \mathcal{N}_\infty(\epsilon, \Theta),$$

and

$$\mathcal{J}_\square(N, \Theta, F, 8LM, 2\sqrt{2}L\epsilon) \leq \mathcal{J}_\infty(\epsilon, \Theta).$$

□

Assumption E.4 (Convergence of θ_N). *For any $\theta, \theta^* \in \Theta$, define*

$$s_N(\theta, \theta^*) := \sqrt{\frac{1}{N} \sum_{i=1}^N E \left[\phi \left(\frac{f_\theta(O_i, C_i) - f_{\theta^*}(O_i, C_i)}{Z} \right) \mid \bar{O}(i-1) \right]},$$

where $Z = 8LM$. Assume that $s_N(\theta_N, \theta^*) = O_P(\delta_N)$ for some $\delta_N \rightarrow 0$.

Theorem E.2 (Maximal Inequality of a Martingale Process). $\forall x > 0, N \in \mathbb{N}$, and $0 < r < \infty$. Denote $a_N(r, x) := \frac{16Z}{\sqrt{N}} \log \mathcal{N}_\infty \left(\frac{r}{2\sqrt{2}L}, \Theta \right) + 64 \mathcal{J}_\infty \left(\frac{r}{2\sqrt{2}L}, \Theta \right) + 32r\sqrt{x} + \frac{16}{\sqrt{N}} Zx$.

Suppose that Assumptions [E.1](#), [E.2](#), [E.3](#) and [E.4](#) hold. Then,

$$P\left(\sup_{\theta^* \in \Theta} I(s_N(\theta_N, \theta^*) \leq r) \sqrt{N} M_{2,N}(\theta_N, \theta^*) \geq a_N(r, x)\right) \leq 2e^{-x}.$$

Proof. Recall that

$$M_{2,N}(\theta_N, \theta^*) = \frac{1}{N} \sum_{i=1}^N \left\{ f_{\theta_N}(O_i, C_i) - f_{\theta^*}(O_i, C_i) - E \left[f_{\theta_N}(O_i, C_i) - f_{\theta^*}(O_i, C_i) \mid \bar{O}(i-1) \right] \right\}.$$

Let $Z = 8LM$ and $b_N(r, x) = \frac{16Z}{\sqrt{N}} \log \mathcal{N}_{\square}(N, \Theta, F, Z, r) + 64\mathcal{J}_{\square}(N, \Theta, F, Z, r) + 32r\sqrt{x} + \frac{16}{\sqrt{N}}Zx$. We have that

$$\begin{aligned} & P\left(\sqrt{N} M_{2,N}(\theta_N, \theta^*) I(s_N(\theta_N, \theta^*) \leq r) \geq a_N(r, x)\right) \\ & \leq P\left(\sup_{\theta^* \in \Theta} I(s_N(\theta_N, \theta^*) \leq r) \sqrt{N} M_{2,N}(\theta_N, \theta^*) \geq a_N(r, x)\right) \\ & \leq P\left(\sup_{\theta^* \in \Theta} I(s_N(\theta_N, \theta^*) \leq r) \sqrt{N} M_{2,N}(\theta_N, \theta^*) \geq b_N(r, x)\right) \\ & \leq 2e^{-x}, \end{aligned}$$

where the second inequality is given by Lemma [E.1](#) and the third inequality is based on the maximal inequality for the martingale process in Theorem [E.1](#).

□

Corollary E.1. *Suppose Assumptions [E.1](#), [E.2](#), [E.3](#) and [E.4](#) hold, then $M_{2,N}(\theta_N, \theta^*) = o_P(N^{-\frac{1}{2}})$.*

Proof. Since $s_N(\theta_N, \theta^*) = O_P(\delta_N)$, one can find a $r_N = \delta_N^{1-\rho}$ for some $\rho > 0$ such that

$r_N \rightarrow 0$ and $\sqrt{N}r_N^2 \not\rightarrow 0$. Then for $\forall x > 0$, we have

$$\begin{aligned}
a_N(r_N, x) &= \frac{16Z}{\sqrt{N}} \log \mathcal{N}_\infty \left(\frac{r_N}{2\sqrt{2L}}, \Theta \right) + 64\mathcal{J}_\infty \left(\frac{r_N}{2\sqrt{2L}}, \Theta \right) + 32r_N\sqrt{x} + \frac{16}{\sqrt{N}}Zx \\
&\leq \frac{16Z}{\sqrt{N}} \left(\frac{2\sqrt{2L}}{r_N} \mathcal{J}_\infty \left(\frac{r_N}{2\sqrt{2L}}, \Theta \right) \right)^2 + 64\mathcal{J}_\infty \left(\frac{r_N}{2\sqrt{2L}}, \Theta \right) + 32r_N\sqrt{x} + \frac{16}{\sqrt{N}}Zx \\
&\leq \left(\frac{108L^2Z}{\sqrt{N}r_N^2} \mathcal{J}_\infty \left(\frac{r_N}{2\sqrt{2L}}, \Theta \right) + 64 \right) \mathcal{J}_\infty \left(\frac{r_N}{2\sqrt{2L}}, \Theta \right) + 32r_N\sqrt{x} + \frac{16}{\sqrt{N}}Zx \\
&\rightarrow 0.
\end{aligned}$$

Thus, $\forall y > 0$, there exists a $N_1 > 0$, such that for every $N > N_1$,

$$\begin{aligned}
&P(\sqrt{N}M_{2,N}(\theta_N, \theta^*)I(s_N(\theta_N, \theta^*) \leq r_N) > y) \\
&\leq P\left(\sup_{\theta^* \in \Theta} I(s_N(\theta_N, \theta^*) \leq r_N) \sqrt{N}M_{2,N}(\theta_N, \theta^*) \geq a_N(r_N, x)\right) \\
&\leq 2e^{-x},
\end{aligned}$$

where the last inequality is implied by Theorem E.2. Similarly, $\forall x > 0, y > 0$, there exists a $N_2 > 0$, such that for every $N > N_2$, $P(-\sqrt{N}M_{2,N}(\theta_N, \theta^*)I(s_N(\theta_N, \theta^*) \leq r_N) > y) \leq 2e^{-x}$. Since $P(s_N(\theta_N, \theta^*) \leq r_N) \rightarrow 1$, we have that $\sqrt{N}M_{2,N}(\theta_N, \theta^*) = o_P(1)$. \square

As introduced in Appendix B, van der Laan (2023) proved the supremum-norm covering number for the class of functions $D^{(m)}([0, 1]^d)$ for $(m = 1, 2, \dots)$, which implies a bound on its uniform entropy integral $J_\infty(r, D^{(m)}([0, 1]^d)) \asymp r^{(2m+1)/(2m+2)}(-\log r)^{d-\frac{3}{2}}$. The m -th order HAL-MLEs are also defined, with the uniform convergence rate of $N^{-\frac{m+1}{2m+3}}$, up to logarithmic factors. Using these theoretical results, we provide another corollary which shows that if θ^* lies in $D^{(m)}([0, 1]^d)$ ($m = 1, 2, 3, \dots$) and θ_N is an estimate of θ^* by higher-order spline HAL-MLE, then the equicontinuity result for the martingale process $M_{2,N}$ holds.

Assumption E.5. Suppose that $\theta^* \in D^{(m)}([0, 1]^d)$ and $\theta_N \in D^{(m)}([0, 1]^d)$ is estimated by

the m -order spline HAL-MLE ($m = 1, 2, \dots$).

Corollary E.2. *Suppose Assumptions E.2, E.3 and E.5 hold, then $M_{2,N}(\theta_N, \theta^*) = o_P(N^{-\frac{1}{2}})$.*

Proof. Let $N_\infty(r, D^{(m)}([0, 1]^d))$ denote the number of spheres of size r w.r.t. supremum norm that are needed to cover $D^{(m)}([0, 1]^d)$. Define $J_\infty(r, D^{(m)}([0, 1]^d))$ as the corresponding supremum norm entropy integral of $D^{(m)}([0, 1]^d)$. In van der Laan (2023), Lemma 29 shows that $J_\infty(r, D^{(m)}([0, 1]^d)) \asymp r^{(2m+1)/(2m+2)}(-\log r)^{d-\frac{3}{2}}$, which implies $J_\infty(r_N, D^{(m)}([0, 1]^d)) \rightarrow 0$ for any $r_N \rightarrow 0$ and satisfies Assumption E.1; Theorem 12 proves the uniform convergence rate $\|\theta_N - \theta^*\|_\infty = O_P(N^{-\frac{m+1}{2m+3}} \log^{c_1} N)$ for some $c_1 < \infty$, which satisfies Assumption E.4. Therefore, together with E.2 and E.3, one can apply Corollary E.1 to prove that $M_{2,N}(\theta_N, \theta^*) = o_P(N^{-\frac{1}{2}})$. \square

F Proof of Equicontinuity Result in Adaptive Designs

Recall that in Section 4

$$M_{2,n_t}(\bar{Q}_{n,K,t}^*, \bar{Q}_{1,K}) = \frac{1}{n_t} \sum_{i=1}^{n_t} \left\{ \left[D_k(\bar{Q}_{n,K,t}^*)(O_i, C_i) - E[D_k(\bar{Q}_{n,K,t}^*)(O_i, C_i) | \mathcal{H}(i)] \right] \right. \\ \left. - \left[D_k(\bar{Q}_{1,K})(O_i, C_i) - E[D_k(\bar{Q}_{1,K})(O_i, C_i) | \mathcal{H}(i)] \right] \right\},$$

where $D_k(\bar{Q}_K)(O_i, C_i) := \frac{g_{k,i}^*(A_i|C_i)}{g_{0,i}(A_i|C_i)} (Y_{i,K} - \bar{Q}_K(A_i, W_i))$. We apply the general results in Appendix E to prove the equicontinuity condition $M_{2,n_t}(\bar{Q}_{n,K,t}^*, \bar{Q}_{1,K}) = o_P(n_t^{-\frac{1}{2}})$ in Theorem 4 and Corollary 1 in the context of adaptive designs.

Proof of Theorem 4 and Corollary 1. Let $\Theta = \bar{Q}_K$, $f_\theta = D_k(\bar{Q}_K)$, $\theta^* = \bar{Q}_{1,K}$, $N = n_t$, $\theta_N = \bar{Q}_{n,K,t}$ in the general setup in Appendix E. Under Assumption 4, $\zeta < g_{0,i} < 1 - \zeta$ and $\zeta < g_{k,i}^* < 1 - \zeta$. Since Y_K and Q_K take values in the interval $[0, 1]$, we have that

$\sup_{\bar{Q}_K \in \bar{\mathcal{Q}}_K} \|D_k(\bar{Q}_K)\|_\infty \leq \frac{2(1-\zeta)}{\zeta} < \infty$, $\sup_{\bar{Q}_{K,1} \in \bar{\mathcal{Q}}_K, \bar{Q}_{K,2} \in \bar{\mathcal{Q}}_K, \bar{Q}_{K,1} \neq \bar{Q}_{K,2}} \frac{\|D_k(\bar{Q}_{K,1}) - D_k(\bar{Q}_{K,2})\|_\infty}{\|\bar{Q}_{K,1} - \bar{Q}_{K,2}\|_\infty} \leq \frac{1-\zeta}{\zeta} < \infty$. Therefore, Assumptions E.2 and E.3 are satisfied. Since Assumption 7 serves as an analog in our adaptive design framework to Assumption E.4 in the general framework, we can utilize Corollary E.1 to demonstrate that $M_{2,n_t}(\bar{Q}_{n,K,t}^*, \bar{Q}_{1,K}) = o_P\left(n_t^{-\frac{1}{2}}\right)$. Similarly, Assumption 8 parallels Assumption E.5 in Corollary E.2. Therefore, Corollary 1 is a specification of Corollary E.2 within our adaptive design setup, which implies $s_{n_t}(\bar{Q}_{n,K,t}, \bar{Q}_{1,K}) = O_P(\delta_{n_t})$ where δ_{n_t} is the HAL convergence rate and preserved by $s_{n_t}(\bar{Q}_{n,K,t}^*, \bar{Q}_{1,K})$ with the TMLE update $\bar{Q}_{n,K,t}^*$. This results in the equicontinuity condition $M_{2,n_t}(\bar{Q}_{n,K,t}^*, \bar{Q}_{1,K}) = o_P\left(n_t^{-\frac{1}{2}}\right)$. \square

G Additional Results for Section 5

The data generating distributions of the two simulation scenarios in Section 5 are as follows. The baseline covariate W follows a uniform distribution $U(-4, 4)$. In Scenario 1, the conditional mean functions of Y_k given A and W are $E[Y_k|A, W] = (2A - 1) \times [0.5 - (1 + \exp(-(3 - k) - W))^{-1}]$. In Scenario 2, the conditional mean functions of Y_k are $E[Y_k|A, W] = (2A - 1) \times [0.5 - (1 + \exp(-\gamma_k W))^{-1}]$, where $\gamma_1 = 3, \gamma_2 = 2, \gamma_3 = 1, \gamma_4 = 0.5$ and $\gamma_5 = 0.25$. The treatment randomization probability of binary treatment $A \in \{0, 1\}$ depends on the configuration of each design.

In simulation studies, we estimate these conditional mean functions using Super Learner (van der Laan et al., 2007), which includes Random Forest (Breiman, 2001), XGBoost (Chen and Guestrin, 2016), the first-order Highly Adaptive Lasso (HAL) estimator (van der Laan, 2023) and an intercept model in the library. The CATE functions and their pointwise confidence intervals are estimated using the first-order HAL, as described in Appendix C.

Tables S1, S2 and S3 report bias, variance of TMLE and coverage probabilities of TMLE-

based confidence intervals for estimating $\Psi_{t,k}$. Tables S4 and S5 report the probability of allocating suboptimal treatment assignment and the average regret, respectively. The trajectory of regret over time is presented in Figure S1. The TMLE results of the proposed adaptive-design estimands $\Psi_{T_{end},k}$ at the end of the experiment are given by Table S6.

Table S1: Bias ($\times 10^{-3}$) of TMLE estimators for $\Psi_{t,k}$ in Scenarios 1 and 2 ($t = 11, 21, 31, 41, 50$).

(a) Scenario 1							(b) Scenario 2						
t	$\Psi_{t,RCT}$	$\Psi_{t,1}$	$\Psi_{t,2}$	$\Psi_{t,3}$	$\Psi_{t,4}$	$\Psi_{t,5}$	t	$\Psi_{t,RCT}$	$\Psi_{t,1}$	$\Psi_{t,2}$	$\Psi_{t,3}$	$\Psi_{t,4}$	$\Psi_{t,5}$
11	-0.77	-1.84	-2.76	-2.96	-2.47	-1.15	11	-1.56	0.26	-0.60	-0.57	-1.52	-2.17
21	-1.36	-3.34	-3.79	-3.32	-1.12	-0.01	21	-3.36	-1.87	-1.62	-2.23	-2.17	-2.83
31	-5.17	-6.20	-4.99	-3.63	-1.66	-2.36	31	-2.37	-0.51	-0.25	-0.57	-0.56	-0.83
41	-4.00	-4.19	-2.89	-1.29	-0.39	-1.31	41	-1.33	0.29	0.45	0.41	0.52	0.13
50	-1.38	-0.06	-0.51	-0.26	0.92	-0.87	50	1.29	1.13	1.35	1.22	1.16	1.50

Table S2: Variance ($\times 10^{-3}$) of TMLE estimators for $\Psi_{t,k}$ in Scenarios 1 and 2 ($t = 11, 21, 31, 41, 50$).

(a) Scenario 1							(b) Scenario 2						
t	$\Psi_{t,RCT}$	$\Psi_{t,1}$	$\Psi_{t,2}$	$\Psi_{t,3}$	$\Psi_{t,4}$	$\Psi_{t,5}$	t	$\Psi_{t,RCT}$	$\Psi_{t,1}$	$\Psi_{t,2}$	$\Psi_{t,3}$	$\Psi_{t,4}$	$\Psi_{t,5}$
11	3.44	7.49	5.55	4.88	4.17	3.83	11	3.11	4.84	4.55	4.09	3.55	3.32
21	2.45	4.21	2.93	2.36	1.85	2.23	21	2.23	1.51	1.49	1.45	1.50	1.94
31	1.75	3.47	2.23	1.67	1.19	1.29	31	1.56	0.83	0.83	0.80	0.87	1.09
41	1.28	2.66	1.74	1.31	0.89	0.90	41	1.18	0.60	0.59	0.59	0.67	0.76
50	1.06	2.35	1.47	1.10	0.70	0.68	50	0.94	0.44	0.45	0.45	0.51	0.59

Table S3: Coverage probability (%) of confidence intervals for $\Psi_{t,k}$ in Scenarios 1 and 2 ($t = 11, 21, 31, 41, 50$).

(a) Scenario 1							(b) Scenario 2						
t	$\Psi_{t,RCT}$	$\Psi_{t,1}$	$\Psi_{t,2}$	$\Psi_{t,3}$	$\Psi_{t,4}$	$\Psi_{t,5}$	t	$\Psi_{t,RCT}$	$\Psi_{t,1}$	$\Psi_{t,2}$	$\Psi_{t,3}$	$\Psi_{t,4}$	$\Psi_{t,5}$
11	96.2	95.0	95.8	96.2	96.2	95.6	11	95.4	95.6	95.4	95.4	95.8	95.2
21	93.8	94.0	94.8	94.6	94.2	94.2	21	94.6	96.4	96.0	95.4	95.2	95.2
31	94.0	92.0	94.4	95.2	95.4	94.2	31	94.6	95.8	95.6	96.4	95.6	95.2
41	94.4	93.2	94.6	94.4	95.2	94.0	41	94.4	94.8	95.4	95.8	96.0	95.4
50	95.0	93.4	96.6	96.6	94.0	95.2	50	96.0	96.6	96.8	97.0	96.4	96.0

Table S4: Probability (%) of not assigning optimal personalized treatments in Scenarios 1 and 2 ($t = 11, 21, 31, 41, 50$). $p_t^{non-opt} := \frac{1}{E(t)} \sum_{i:t_i=t} I(A_i \neq d_{0,K}(W_i))$, where $d_{0,K}(W) := I(\bar{Q}_{0,K}(1, W) - \bar{Q}_{0,K}(0, W) > 0)$

(a) Scenario 1								(b) Scenario 2							
t	$p_{t,SL}^{non-opt}$	$p_{t,1}^{non-opt}$	$p_{t,2}^{non-opt}$	$p_{t,3}^{non-opt}$	$p_{t,4}^{non-opt}$	$p_{t,5}^{non-opt}$	$p_{t,RCT}^{non-opt}$	t	$p_{t,SL}^{non-opt}$	$p_{t,1}^{non-opt}$	$p_{t,2}^{non-opt}$	$p_{t,3}^{non-opt}$	$p_{t,4}^{non-opt}$	$p_{t,5}^{non-opt}$	$p_{t,RCT}^{non-opt}$
11	28.4	51.4	39.7	30.0	20.1	15.9	49.9	11	15.3	14.0	14.6	16.2	19.5	30.9	50.3
21	20.2	50.8	40.1	30.0	20.6	14.7	49.8	21	13.4	12.7	13.1	14.4	16.6	24.5	50.2
31	17.5	50.1	39.8	29.8	20.3	14.1	50.0	31	12.8	12.3	12.7	13.9	15.7	21.6	49.4
41	14.9	49.9	40.0	30.1	19.7	13.0	50.1	41	11.9	11.7	11.9	13.0	15.0	19.3	50.8
50	14.9	50.1	39.8	29.6	19.9	13.2	50.5	50	12.1	11.5	12.0	12.6	14.4	18.6	50.5

Table S5: Average regret of not selecting optimal personalized treatments in Scenarios 1 and 2 ($t = 11, 21, 31, 41, 50$).

(a) Scenario 1								(b) Scenario 2							
t	$R_{t,SL}$	$R_{t,1}$	$R_{t,2}$	$R_{t,3}$	$R_{t,4}$	$R_{t,5}$	$R_{t,RCT}$	t	$R_{t,SL}$	$R_{t,1}$	$R_{t,2}$	$R_{t,3}$	$R_{t,4}$	$R_{t,5}$	$R_{t,RCT}$
11	0.154	0.348	0.240	0.160	0.099	0.083	0.344	11	0.030	0.027	0.028	0.029	0.035	0.064	0.121
21	0.102	0.340	0.241	0.159	0.101	0.080	0.341	21	0.026	0.026	0.026	0.027	0.030	0.048	0.121
31	0.088	0.337	0.241	0.158	0.100	0.078	0.342	31	0.025	0.025	0.026	0.026	0.028	0.040	0.119
41	0.078	0.331	0.238	0.156	0.093	0.071	0.343	41	0.024	0.025	0.025	0.025	0.027	0.035	0.122
50	0.077	0.336	0.240	0.155	0.096	0.074	0.348	50	0.023	0.024	0.024	0.025	0.027	0.033	0.121

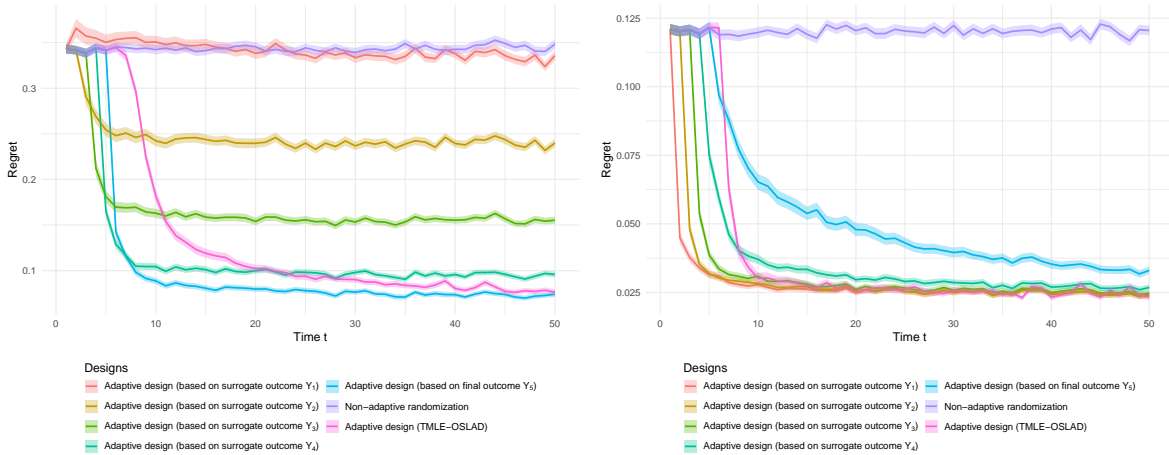


Figure S1: Regret at time t for different design strategies in Scenario 1 (left) and Scenario 2 (right). This figure includes seven curves: five curves correspond to regrets from adaptive designs using outcomes from Y_1 to Y_5 , respectively; one curve illustrates the regret for an adaptive design employing a TMLE-OSLAD to evaluate and utilize surrogates; and the last curve represents the regret of a fixed design, which assigns equal probabilities to each treatment group. The shaded regions represent twice the standard error of the regret across simulations.

Table S7 reports the true expected final outcome Y_5 obtained from implementing different adaptive designs at illustrative time points $t = 11, 21, 31, 41, 50$, respectively. These

Table S6: Performance of TMLE estimators for the proposed adaptive-design estimands at the end of experiments in Scenarios 1 and 2.

(a) Scenario 1						
Estimand	Notation	Truth	Bias ($\times 10^{-3}$)	Var ($\times 10^{-3}$)	Coverage (%)	
Expected Final Outcome Y_5 under adaptive design using Y_1	$\psi_{T_{end},1}$	0.018	0.21	2.08	94.6	
Expected Final Outcome Y_5 under adaptive design using Y_2	$\psi_{T_{end},2}$	0.095	-0.29	1.36	94.6	
Expected Final Outcome Y_5 under adaptive design using Y_3	$\psi_{T_{end},3}$	0.174	-0.59	0.97	96.0	
Expected Final Outcome Y_5 under adaptive design using Y_4	$\psi_{T_{end},4}$	0.223	-0.16	0.62	95.4	
Expected Final Outcome Y_5 under adaptive design using Y_5	$\psi_{T_{end},5}$	0.237	-0.18	0.60	95.6	

(b) Scenario 2						
Estimand	Notation	Truth	Bias ($\times 10^{-3}$)	Var ($\times 10^{-3}$)	Coverage (%)	
Expected Final Outcome Y_5 under adaptive design using Y_1	$\psi_{T_{end},1}$	0.092	1.26	0.41	96.4	
Expected Final Outcome Y_5 under adaptive design using Y_2	$\psi_{T_{end},2}$	0.090	1.43	0.41	97.4	
Expected Final Outcome Y_5 under adaptive design using Y_3	$\psi_{T_{end},3}$	0.087	1.41	0.41	97.0	
Expected Final Outcome Y_5 under adaptive design using Y_4	$\psi_{T_{end},4}$	0.081	1.30	0.46	97.2	
Expected Final Outcome Y_5 under adaptive design using Y_5	$\psi_{T_{end},5}$	0.065	1.70	0.52	96.6	

values represent the ideal estimand as discussed in Appendix A.2. We use $\tilde{\Psi}_{t,k}$ to denote the ideal estimand under the adaptive design guided by surrogate Y_k . We further use $\tilde{\Psi}_{t,RCT}$ and $\tilde{\Psi}_{t,SL}$ to denote the true expected final outcomes obtained from implementing the non-adaptive RCT and our proposed TMLE-OSLAD design, respectively. Comparing with the proposed context-specific estimands $\Psi_{t,k}$ in Table 1, the two estimands show minimal discrepancy, and the relative superiority between different surrogate-guided designs remains unchanged.

Table S7: True expected final outcome $\tilde{\Psi}_{t,k}$ under different adaptive designs in Scenarios 1 and 2 ($t = 11, 21, 31, 41, 50$).

(a) Scenario 1								(b) Scenario 2							
t	$\tilde{\Psi}_{t,RCT}$	$\tilde{\Psi}_{t,1}$	$\tilde{\Psi}_{t,2}$	$\tilde{\Psi}_{t,3}$	$\tilde{\Psi}_{t,4}$	$\tilde{\Psi}_{t,5}$	$\tilde{\Psi}_{t,SL}$	t	$\tilde{\Psi}_{t,RCT}$	$\tilde{\Psi}_{t,1}$	$\tilde{\Psi}_{t,2}$	$\tilde{\Psi}_{t,3}$	$\tilde{\Psi}_{t,4}$	$\tilde{\Psi}_{t,5}$	$\tilde{\Psi}_{t,SL}$
11	0.000	-0.011	0.052	0.077	0.065	0.033	0.000	11	0.000	0.070	0.056	0.039	0.018	0.004	0.000
21	0.000	-0.007	0.081	0.142	0.174	0.171	0.100	21	0.000	0.084	0.079	0.071	0.059	0.036	0.054
31	0.000	-0.003	0.090	0.160	0.201	0.207	0.155	31	0.000	0.089	0.085	0.080	0.071	0.051	0.069
41	0.000	0.000	0.094	0.167	0.214	0.224	0.183	41	0.000	0.090	0.088	0.084	0.077	0.059	0.076
50	0.000	0.001	0.096	0.171	0.221	0.233	0.199	50	0.000	0.091	0.089	0.086	0.080	0.064	0.080

H Sensitivity Analyses

We further conduct a series of sensitivity analyses to compare the performance of TMLE-OSLAD across different design configurations.

First, we perform sensitivity analyses to assess how TMLE-OSLAD’s surrogate selection pattern changes with different α ’s used in (i) the $100(1 - \alpha)\%$ TMLE-based Wald-type confidence interval for evaluating and choosing from candidate designs, and (ii) the $100(1 - \alpha)\%$ CATE confidence intervals for generating treatment randomization probabilities. Figures S2 and S3 report the selection frequency of each surrogate-guided design at each time point when the TMLE-based selection criterion, originally based on 95% CIs, is re-evaluated using 90% and 99% confidence intervals. The selection patterns remain consistent across these choices, with only a slight decrease in the selection probability of Y_5 as the CI level increases in Scenario 1.

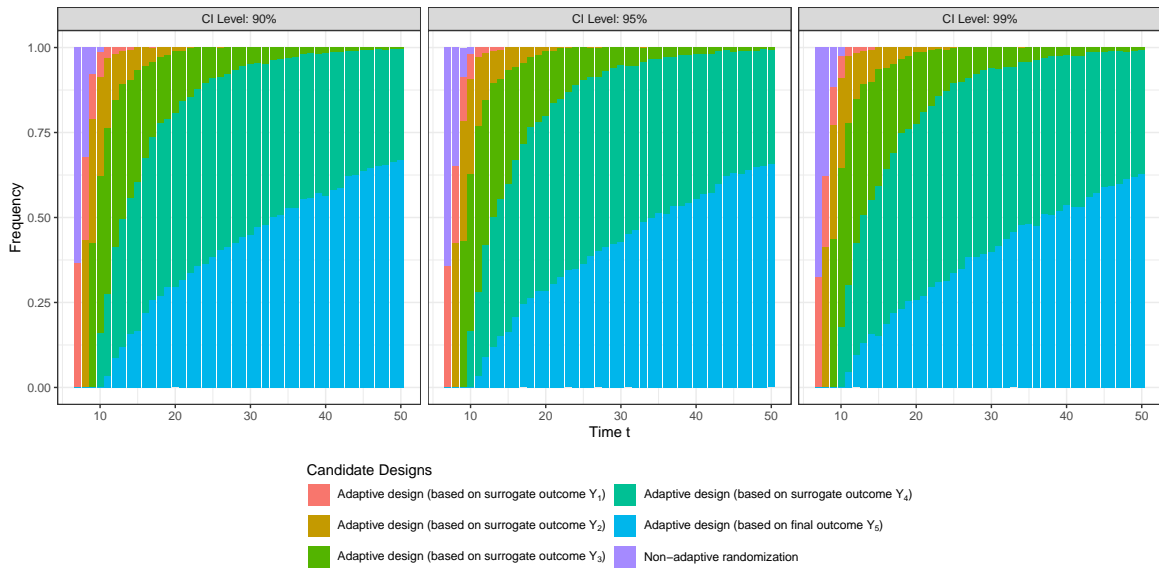


Figure S2: Frequency of candidate designs selected by TMLE-OSLAD using different TMLE confidence interval levels in Scenario 1.

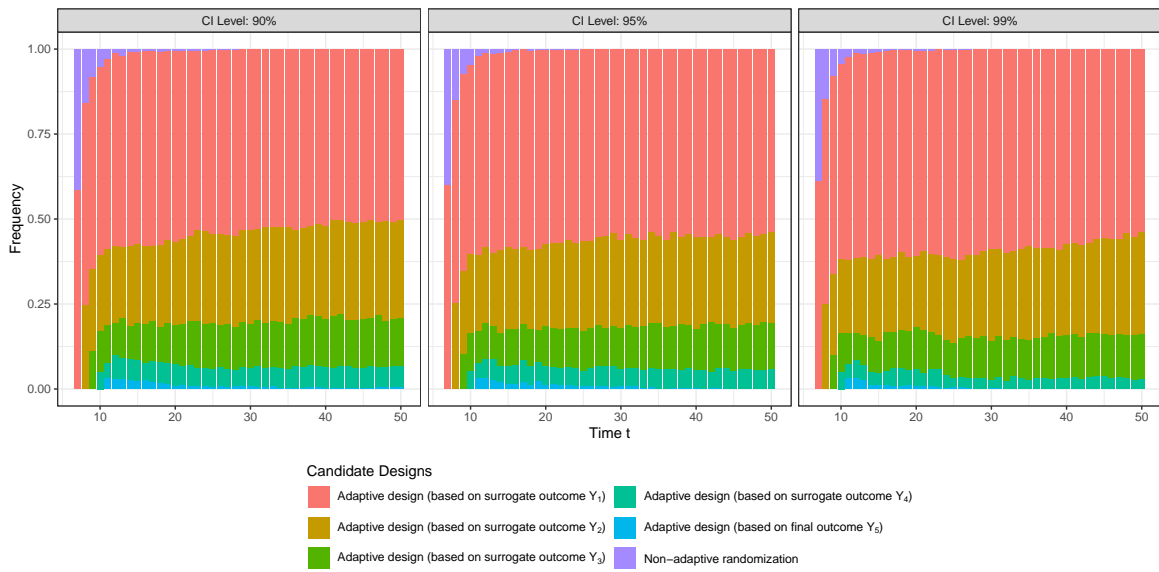


Figure S3: Frequency of candidate designs selected by TMLE-OSLAD using different TMLE confidence interval levels in Scenario 2.

Figures S4 and S5 report the selection frequency of each candidate surrogate-driven design obtained by implementing adaptive designs where treatment-randomization probabilities are based upon $100(1 - \alpha)\%$ CATE confidence intervals with $\alpha \in \{0.01, 0.05, 0.10\}$ for Scenarios 1 and 2, respectively. The selection patterns are consistent across different CI levels, with only a slight increase in the selection probability of Y_1 in Scenario 2 as the CI level rises.

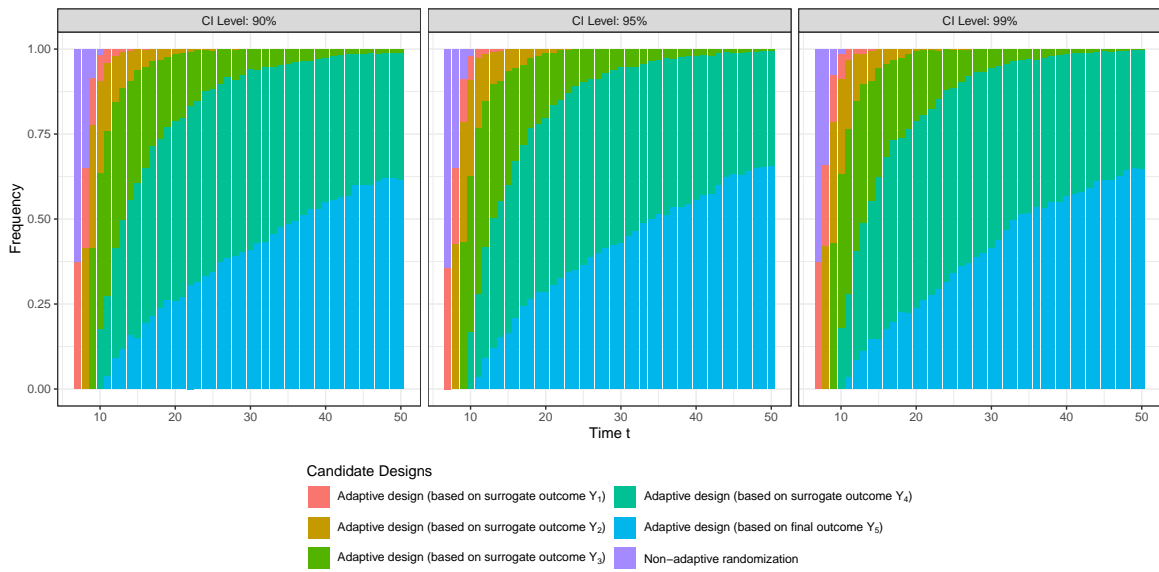


Figure S4: Frequency of candidate designs selected by TMLE-OSLAD using different levels of CATE confidence interval to adapt treatment randomization probabilities in Scenario 1.

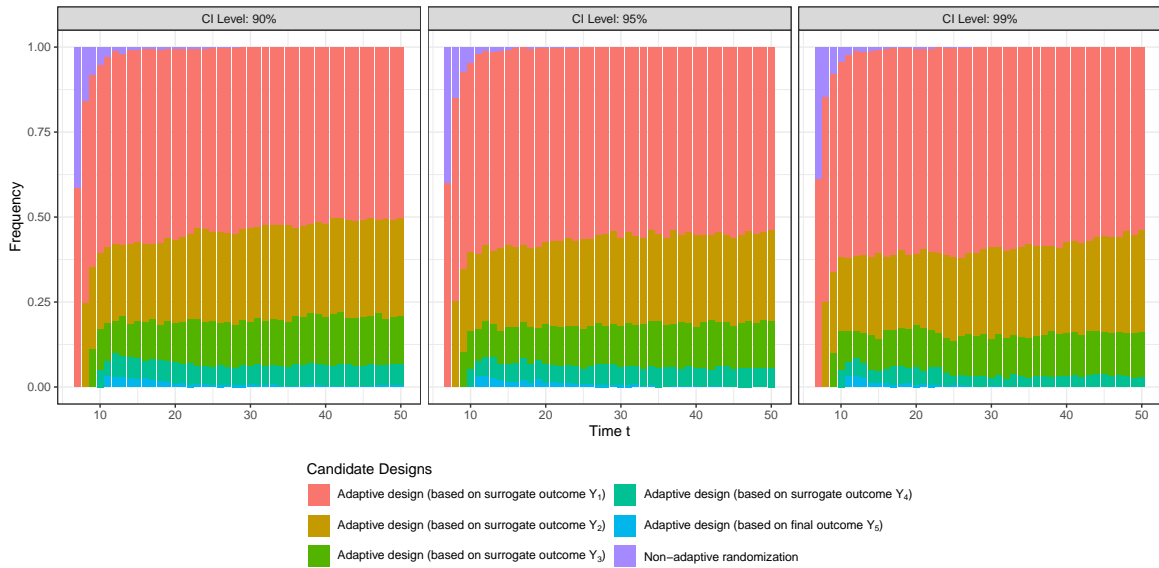


Figure S5: Frequency of candidate designs selected by TMLE-OSLAD using different levels of CATE confidence interval to adapt treatment randomization probabilities in Scenario 2.

Second, we conduct a sensitivity analysis on our proposed TMLE-OSLAD design with a different choice of h_{ν} . As noted in Appendix D, the treatment randomization probabilities

we use is

$$h_\nu(z) = \begin{cases} \nu, & z \leq -1 \\ \nu + (1 - 2\nu) \left(-\frac{1}{4}z^3 + \frac{3}{4}z + \frac{1}{2} \right), & -1 < z < 1, \\ 1 - \nu, & z \geq 1 \end{cases} \quad (1)$$

where the input z is the ratio of the CATE estimate to half the width of its $100(1 - \alpha)\%$ confidence interval. Let $f^{(0)}$ denote the function used in the second term of h_ν for $-1 < z < 1$, defined as $f^{(0)}(z) = -\frac{1}{4}z^3 + \frac{3}{4}z + \frac{1}{2}$. To examine the sensitivity of our proposed methods to different treatment randomization schemes, we consider three additional functions that vary in how aggressively the estimated CATE signal is transformed into a skewed treatment randomization probability favoring the estimated optimal personalized treatment. These functions are defined as follows: (i) $f^{(1)}(z) = 1/(1 + \exp(-8z))$, (ii) $f^{(2)}(z) = \frac{1}{4}z^3 + \frac{1}{4}z + \frac{1}{2}$, and (iii) $f^{(3)}(z) = -\frac{1}{4}z^5 + \frac{3}{4}z^3 + \frac{1}{2}$. To facilitate comparison, we use $h_\nu^{(0)}$ to denote the baseline mapping function h_ν in the main text. We then define $h_\nu^{(1)}(z)$, $h_\nu^{(2)}(z)$, and $h_\nu^{(3)}(z)$ as alternative mapping functions that replace $f^{(0)}(z)$ with $f^{(1)}(z)$, $f^{(2)}(z)$, and $f^{(3)}(z)$ for $-1 < z < 1$, respectively. Figure S6 compares the four functions. Relative to $h_\nu^{(0)}$, $h_\nu^{(1)}$ shifts the treatment randomization probability toward the estimated optimal treatment more rapidly as CATE increases, while $h_\nu^{(2)}$ adjusts more gradually, and $h_\nu^{(3)}$ exhibits the slowest transition.

Tables S8 and S9 report the true target estimand $\Psi_{t,k}$ for each surrogate-specific adaptive design under the different mapping functions $h_\nu^{(0)}$ through $h_\nu^{(3)}$. The oracle surrogate that yields the highest target estimand is consistent across different mapping functions. Figures S7 and S8 further show the selection frequency for each candidate design by TMLE-OSLAD across different mapping functions used for treatment randomization. The surrogate selection pattern is robust to the choice of the function, with TMLE-OSLAD consistently identifying

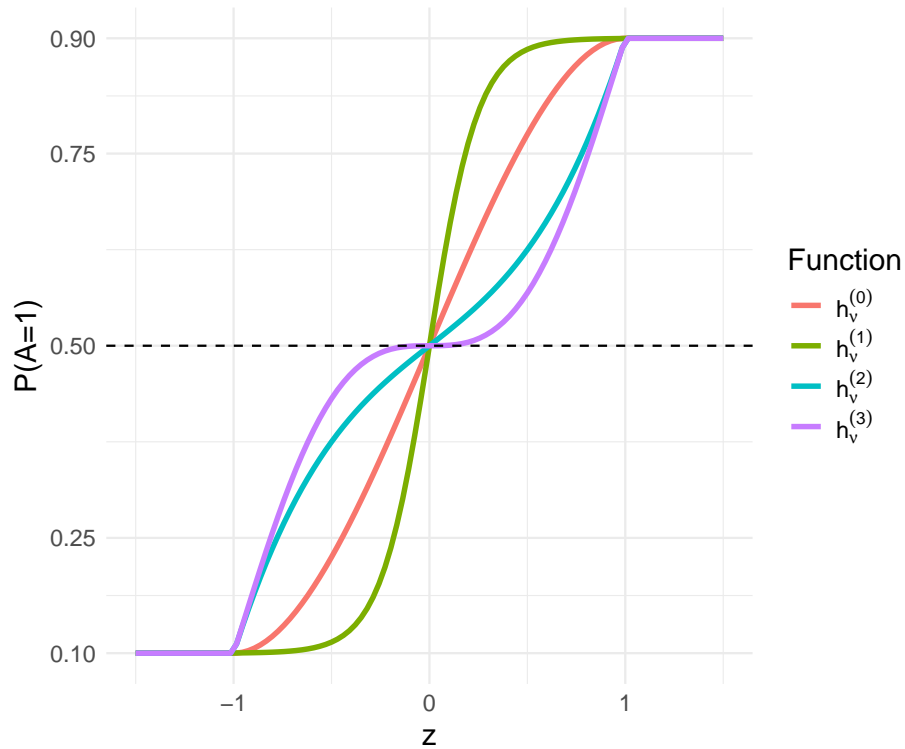


Figure S6: Comparison of the baseline mapping $h_\nu^{(0)}$ and three alternatives $h_\nu^{(1)}$, $h_\nu^{(2)}$, and $h_\nu^{(3)}$ ($\nu = 0.1$) for sensitivity analysis. The x-axis shows the standardized CATE (z), and the y-axis shows the probability of assigning treatment $a = 1$ according to each mapping function (shown as curves).

Table S8: True target estimand $\Psi_{t,k}$ had participants enrolled from $1, \dots, t - K$ were adaptively treated by a candidate surrogate Y_k in Scenarios 1 ($t = 11, 21, 31, 41, 50$) under different mapping functions $h_\nu^{(0)}$ to $h_\nu^{(3)}$. Expected outcomes under the adaptive design using the oracle surrogate are shown in bold.

t	$h_\nu^{(0)}$					$h_\nu^{(1)}$					$h_\nu^{(2)}$					$h_\nu^{(3)}$								
	$\Psi_{t,RCT}$	$\Psi_{t,1}$	$\Psi_{t,2}$	$\Psi_{t,3}$	$\Psi_{t,4}$	$\Psi_{t,5}$	$\Psi_{t,RCT}$	$\Psi_{t,1}$	$\Psi_{t,2}$	$\Psi_{t,3}$	$\Psi_{t,4}$	$\Psi_{t,5}$	$\Psi_{t,RCT}$	$\Psi_{t,1}$	$\Psi_{t,2}$	$\Psi_{t,3}$	$\Psi_{t,4}$	$\Psi_{t,5}$	$\Psi_{t,RCT}$	$\Psi_{t,1}$	$\Psi_{t,2}$	$\Psi_{t,3}$	$\Psi_{t,4}$	$\Psi_{t,5}$
11	0.000	-0.010	0.052	0.077	0.065	0.033	0.000	-0.008	0.055	0.083	0.070	0.036	0.000	-0.011	0.044	0.068	0.058	0.029	0.000	-0.011	0.042	0.065	0.055	0.028
21	0.000	-0.006	0.082	0.144	0.174	0.170	0.000	-0.003	0.085	0.148	0.179	0.175	0.000	-0.008	0.076	0.136	0.166	0.162	0.000	-0.009	0.074	0.134	0.164	0.159
31	0.000	-0.003	0.089	0.160	0.201	0.206	0.000	-0.001	0.092	0.163	0.205	0.210	0.000	-0.007	0.084	0.153	0.194	0.198	0.000	-0.008	0.082	0.151	0.192	0.196
41	0.000	-0.001	0.092	0.168	0.214	0.223	0.000	0.001	0.095	0.171	0.217	0.227	0.000	-0.005	0.088	0.162	0.207	0.216	0.000	-0.005	0.086	0.160	0.206	0.215
50	0.000	0.001	0.094	0.172	0.221	0.233	0.000	0.003	0.097	0.175	0.224	0.236	0.000	-0.003	0.090	0.166	0.215	0.226	0.000	-0.003	0.089	0.165	0.214	0.225

Table S9: True target estimand $\Psi_{t,k}$ had participants enrolled from $1, \dots, t - K$ were adaptively treated by a candidate surrogate Y_k in Scenarios 2 ($t = 11, 21, 31, 41, 50$) under different mapping functions $h_\nu^{(0)}$ to $h_\nu^{(3)}$. Expected outcomes under the adaptive design using the oracle surrogate are shown in bold.

t	$h_\nu^{(0)}$					$h_\nu^{(1)}$					$h_\nu^{(2)}$					$h_\nu^{(3)}$								
	$\Psi_{t,RCT}$	$\Psi_{t,1}$	$\Psi_{t,2}$	$\Psi_{t,3}$	$\Psi_{t,4}$	$\Psi_{t,5}$	$\Psi_{t,RCT}$	$\Psi_{t,1}$	$\Psi_{t,2}$	$\Psi_{t,3}$	$\Psi_{t,4}$	$\Psi_{t,5}$	$\Psi_{t,RCT}$	$\Psi_{t,1}$	$\Psi_{t,2}$	$\Psi_{t,3}$	$\Psi_{t,4}$	$\Psi_{t,5}$	$\Psi_{t,RCT}$	$\Psi_{t,1}$	$\Psi_{t,2}$	$\Psi_{t,3}$	$\Psi_{t,4}$	$\Psi_{t,5}$
11	0.000	0.073	0.057	0.039	0.018	0.004	0.000	0.075	0.059	0.041	0.020	0.004	0.000	0.068	0.052	0.035	0.014	0.003	0.000	0.066	0.051	0.034	0.013	0.003
21	0.000	0.086	0.080	0.072	0.059	0.037	0.000	0.088	0.081	0.074	0.063	0.042	0.000	0.083	0.077	0.069	0.053	0.029	0.000	0.082	0.076	0.068	0.051	0.027
31	0.000	0.089	0.085	0.081	0.071	0.051	0.000	0.091	0.087	0.082	0.074	0.056	0.000	0.087	0.083	0.078	0.065	0.041	0.000	0.086	0.082	0.077	0.063	0.038
41	0.000	0.091	0.088	0.084	0.076	0.058	0.000	0.092	0.089	0.086	0.079	0.064	0.000	0.089	0.086	0.082	0.072	0.048	0.000	0.088	0.085	0.081	0.070	0.045
50	0.000	0.092	0.090	0.086	0.080	0.063	0.000	0.093	0.090	0.088	0.082	0.069	0.000	0.090	0.088	0.084	0.075	0.053	0.000	0.090	0.087	0.084	0.074	0.050

and increasingly favoring the oracle surrogate as the experiment progresses. Moreover, TMLE provides robust inference for these target estimands, with confidence intervals achieving nominal coverage across simulations using different mapping functions (Tables S10 and S11).

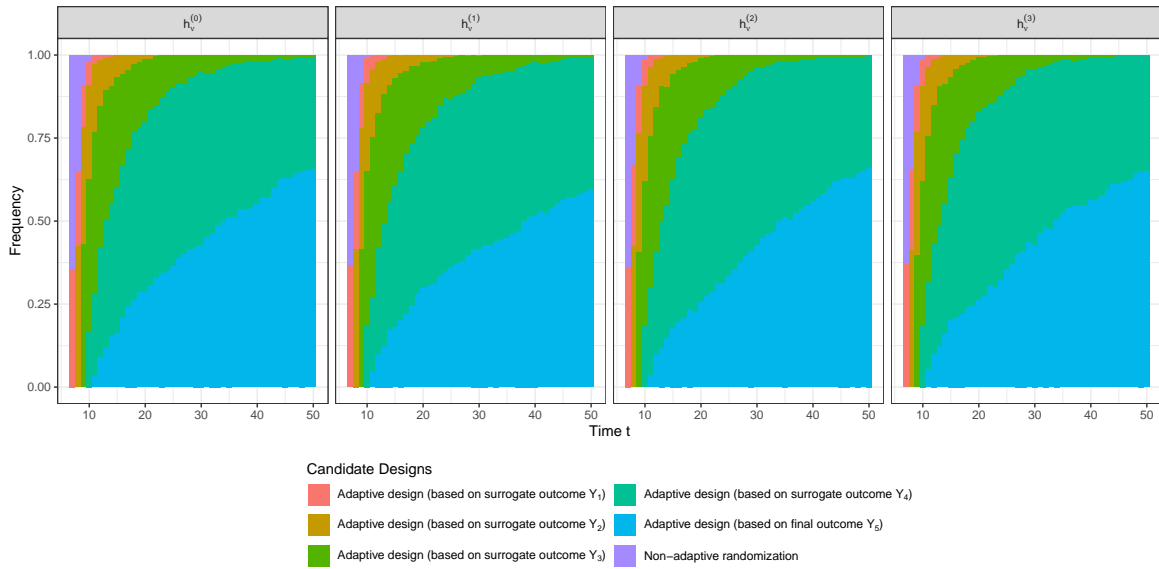


Figure S7: Frequency of candidate designs selected by TMLE-OSLAD under different treatment randomization functions applied in Scenario 1.

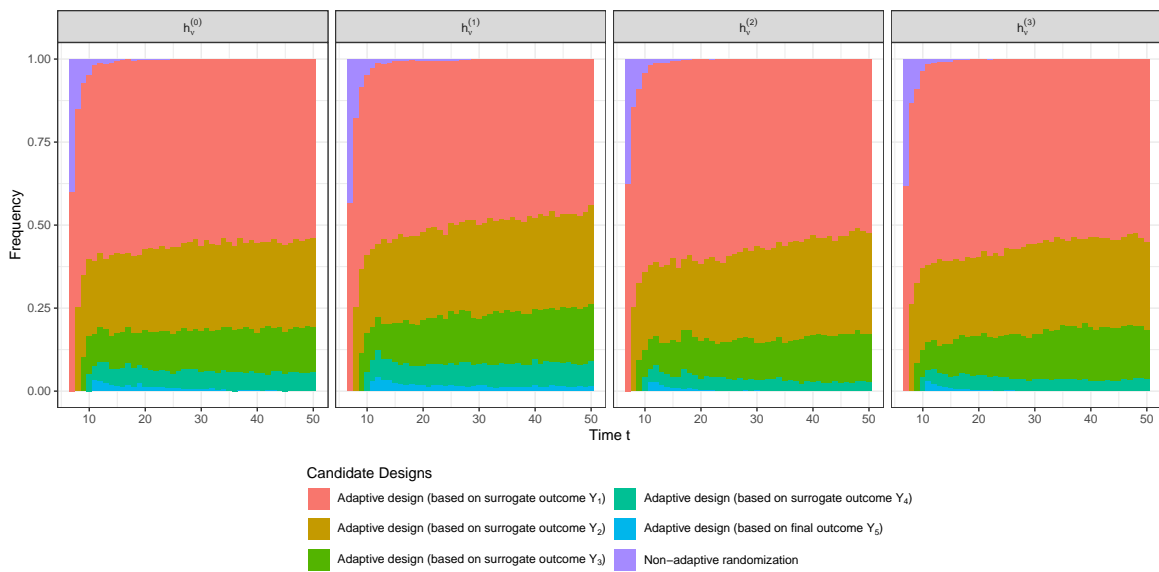


Figure S8: Frequency of candidate designs selected by TMLE-OSLAD under different treatment randomization functions applied in Scenario 2.

Table S10: Coverage probability (%) of confidence interval for target estimands $\Psi_{t,k}$ in Scenarios 1 ($t = 11, 21, 31, 41, 50$) under different mapping functions $h_v^{(0)}$ to $h_v^{(3)}$.

t	$h_v^{(0)}$					$h_v^{(1)}$					$h_v^{(2)}$					$h_v^{(3)}$									
	$\Psi_{t,RCT}$	$\Psi_{t,1}$	$\Psi_{t,2}$	$\Psi_{t,3}$	$\Psi_{t,4}$	$\Psi_{t,5}$	$\Psi_{t,RCT}$	$\Psi_{t,1}$	$\Psi_{t,2}$	$\Psi_{t,3}$	$\Psi_{t,4}$	$\Psi_{t,5}$	$\Psi_{t,RCT}$	$\Psi_{t,1}$	$\Psi_{t,2}$	$\Psi_{t,3}$	$\Psi_{t,4}$	$\Psi_{t,5}$	$\Psi_{t,RCT}$	$\Psi_{t,1}$	$\Psi_{t,2}$	$\Psi_{t,3}$	$\Psi_{t,4}$	$\Psi_{t,5}$	
11	96.2	95.0	95.8	96.2	96.2	95.6	96.8	94.8	95.8	94.8	95.8	96.6	96.8	95.0	95.4	96.2	95.8	97.0	96.8	95.4	95.6	96.6	95.8	96.6	96.6
21	93.8	94.0	94.8	94.6	94.2	94.2	95.0	93.4	94.6	95.4	94.0	94.0	93.8	93.0	94.6	93.4	95.4	93.6	94.0	93.0	95.2	94.0	95.4	93.8	93.8
31	94.0	92.0	94.4	95.2	95.4	94.2	94.4	93.4	94.8	93.8	93.2	93.2	95.4	94.6	95.2	96.4	97.4	95.0	96.2	94.2	95.0	96.4	96.4	94.8	94.8
41	94.4	93.2	94.6	94.4	95.2	94.0	94.8	94.2	95.2	95.4	93.4	93.4	95.2	95.0	95.6	94.4	95.0	93.6	96.8	94.4	95.0	94.8	94.2	93.0	93.0
50	95.0	93.4	96.6	96.6	94.0	95.2	95.2	95.6	94.8	96.4	94.0	94.0	95.8	94.7	94.5	96.2	95.8	94.9	94.8	94.4	94.8	94.8	94.8	94.8	94.0

Table S11: Coverage probability (%) of confidence interval for target estimands $\Psi_{t,k}$ in Scenarios 2 ($t = 11, 21, 31, 41, 50$) under different mapping functions $h_v^{(0)}$ to $h_v^{(3)}$.

t	$h_v^{(0)}$					$h_v^{(1)}$					$h_v^{(2)}$					$h_v^{(3)}$									
	$\Psi_{t,RCT}$	$\Psi_{t,1}$	$\Psi_{t,2}$	$\Psi_{t,3}$	$\Psi_{t,4}$	$\Psi_{t,5}$	$\Psi_{t,RCT}$	$\Psi_{t,1}$	$\Psi_{t,2}$	$\Psi_{t,3}$	$\Psi_{t,4}$	$\Psi_{t,5}$	$\Psi_{t,RCT}$	$\Psi_{t,1}$	$\Psi_{t,2}$	$\Psi_{t,3}$	$\Psi_{t,4}$	$\Psi_{t,5}$	$\Psi_{t,RCT}$	$\Psi_{t,1}$	$\Psi_{t,2}$	$\Psi_{t,3}$	$\Psi_{t,4}$	$\Psi_{t,5}$	
11	95.4	95.6	95.4	95.4	95.8	95.2	95.6	95.2	94.8	95.2	95.6	95.4	95.6	96.0	95.2	95.0	95.0	95.8	95.6	95.8	95.0	95.4	95.0	96.0	96.0
21	94.6	96.4	96.0	95.4	95.2	95.2	95.0	96.2	95.8	96.2	95.6	96.0	96.0	95.2	95.0	95.0	95.8	96.0	95.0	95.6	95.8	95.0	96.2	96.4	96.4
31	94.6	95.8	95.6	96.4	95.6	95.2	94.2	94.8	95.0	95.6	94.0	95.8	94.8	96.0	95.0	95.8	95.6	95.6	93.6	95.0	94.2	95.0	94.2	95.6	95.6
41	94.4	94.8	95.4	95.8	96.0	95.4	96.8	94.6	96.2	95.4	95.2	95.0	96.2	95.2	94.8	95.8	95.2	95.8	96.8	94.4	95.0	94.8	94.8	95.6	95.6
50	96.0	96.6	96.8	97.0	96.4	96.0	96.2	97.0	97.2	96.2	95.0	96.4	95.8	97.6	96.8	97.0	95.6	97.0	96.0	95.8	96.2	95.4	95.8	95.8	97.0

Lastly, we extend the simulation scenarios to include three covariates to further evaluate the performance of our proposed methods. In Scenario 1, the conditional mean functions of Y_k given A and W are $E[Y_k|A, W_1, W_2, W_3] = (2A - 1) \times [0.5 - (1 + \exp(-(3 - k) - 0.4W_1 - 0.4W_2 - 0.2W_3))^{-1}]$. In Scenario 2, the conditional mean functions of Y_k are $E[Y_k|A, W_1, W_2, W_3] = (2A - 1) \times [0.5 - (1 + \exp(-\gamma_k \times (0.4W_1 + 0.4W_2 + 0.2W_3)))^{-1}]$, where $\gamma_1 = 3, \gamma_2 = 2, \gamma_3 = 1, \gamma_4 = 0.5$ and $\gamma_5 = 0.25$. W_1, W_2 , and W_3 are independent and all follow a uniform distribution $U(-4, 4)$.

Table S12 reports the true target estimand $\Psi_{t,k}$. Table S13 shows the coverage probabilities of TMLE-based confidence intervals for these estimands. Figure S9 plots the probability of each surrogate-driven design being selected over time by TMLE-OSLAD in the two scenarios. Similar to the simulation results in the main paper, TMLE-OSLAD consistently provides valid statistical inference with confidence intervals that achieve nominal coverage and selects the oracle surrogate with high frequency in both scenarios.

Table S12: True target estimand $\Psi_{t,k}$ had participants enrolled from $1, \dots, t - K$ were adaptively treated by a candidate surrogate Y_k in Scenarios 1 and 2 ($t = 11, 21, 31, 41, 50$) with three covariates. Expected outcomes under the adaptive design using the oracle surrogate are shown in bold.

(a) Scenario 1							(b) Scenario 2						
t	$\Psi_{t,RCT}$	$\Psi_{t,1}$	$\Psi_{t,2}$	$\Psi_{t,3}$	$\Psi_{t,4}$	$\Psi_{t,5}$	t	$\Psi_{t,RCT}$	$\Psi_{t,1}$	$\Psi_{t,2}$	$\Psi_{t,3}$	$\Psi_{t,4}$	$\Psi_{t,5}$
11	0.000	-0.181	-0.067	0.041	0.063	0.037	11	0.000	0.034	0.025	0.013	0.005	0.001
21	0.000	-0.214	-0.088	0.096	0.168	0.173	21	0.000	0.043	0.039	0.031	0.020	0.009
31	0.000	-0.222	-0.090	0.110	0.193	0.206	31	0.000	0.046	0.043	0.037	0.026	0.013
41	0.000	-0.225	-0.087	0.114	0.205	0.221	41	0.000	0.048	0.045	0.040	0.030	0.016
50	0.000	-0.227	-0.085	0.116	0.211	0.229	50	0.000	0.049	0.047	0.042	0.032	0.018

Table S13: Coverage probability (%) of confidence intervals for $\Psi_{t,k}$ in Scenarios 1 and 2 ($t = 11, 21, 31, 41, 50$) with three covariates.

(a) Scenario 1							(b) Scenario 2						
t	$\Psi_{t,RCT}$	$\Psi_{t,1}$	$\Psi_{t,2}$	$\Psi_{t,3}$	$\Psi_{t,4}$	$\Psi_{t,5}$	t	$\Psi_{t,RCT}$	$\Psi_{t,1}$	$\Psi_{t,2}$	$\Psi_{t,3}$	$\Psi_{t,4}$	$\Psi_{t,5}$
11	94.0	94.2	93.2	94.0	93.8	94.2	11	93.8	93.2	95.2	94.4	93.0	94.0
21	93.2	91.4	91.2	92.4	96.4	95.4	21	94.0	93.8	95.4	93.4	93.8	94.0
31	93.4	92.0	93.2	94.2	96.2	95.2	31	95.2	93.8	94.8	93.2	95.8	95.0
41	95.2	94.8	95.2	92.4	95.4	94.6	41	95.0	94.4	93.8	94.2	94.4	95.6
50	93.8	95.6	93.4	92.0	95.0	96.2	50	95.6	95.4	94.8	94.0	95.6	95.4

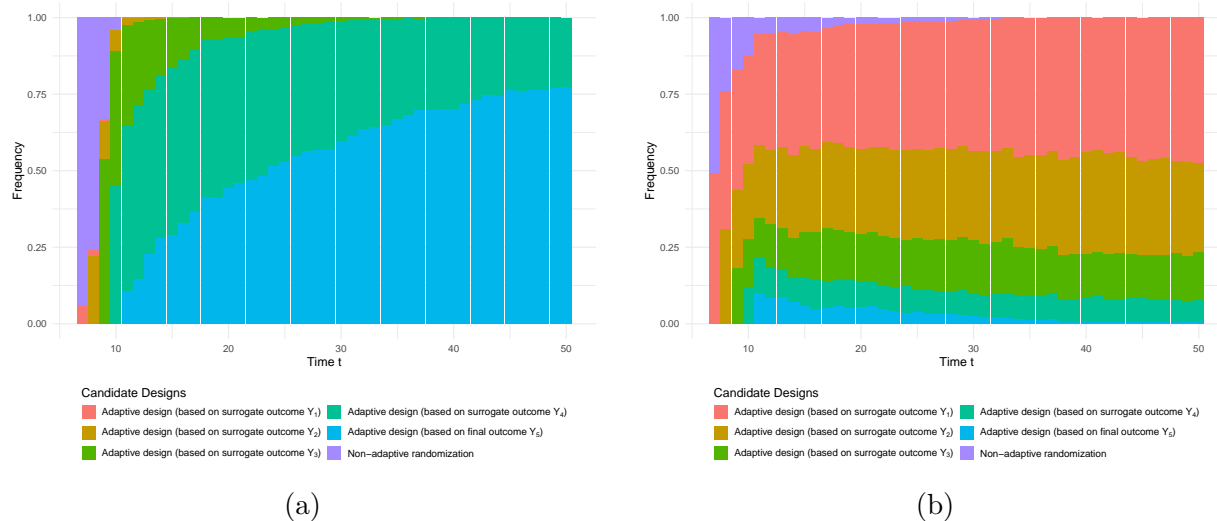


Figure S9: Frequency of candidate adaptive design selected by TMLE-OSLAD at each time point. Panels (a) and (b) correspond to Scenario 1 and Scenario 2 with three covariates.

I Additional Results for Section 6

In this section, we present additional results in ADAPT-R simulation. Figure S10 shows the true CATE functions of Navigator vs. SMS+CCT in ADAPT-R simulation. For participants initially assigned to SMS, the optimal personalized treatment varies with time-to-lapse after initial treatment and shows different patterns across outcomes. For earlier outcomes (Y_1 through Y_3), the CATE suggests that Navigator is preferable with shorter time-to-lapse, but the benefit wanes over time, shifting the optimal treatment to SMS+CCT. In contrast, for later outcomes (Y_4 and Y_5), SMS+CCT is preferred for short time-to-lapse, with their

effectiveness decreasing over time, making Navigator the optimal choice for longer time-to-lapse. For participants whose initial treatment was SOC, the treatment effects are minimal: CATE remains close to zero over the entire range of time-to-lapse periods, indicating small differences between Navigator and SMS+CCT. For participants with CCT as their initial strategy, Navigator is preferred for participants with short time-to-lapse periods, showing a positive CATE. However, as time-to-lapse increases, SMS+CCT becomes increasingly favored, with the CATE decreasing and turning negative.

Figure S11 illustrates regret over time obtained from implementing different design strategies. Table S14 shows the true values of the proposed adaptive-design target estimand $\Psi_{t,k}$ at the illustrative time points 11, 13, 15, 17, and 19, along with the coverage probabilities of the confidence intervals based on TMLE. Table S15 reports the bias and variance of TMLE at these time points. Table S16 presents TMLE’s performance in estimating the proposed adaptive-design estimands at the end of the experiment. Table S17 presents TMLE’s performance of estimating ATE on final outcome and mean final outcome of optimal treatment rules based on surrogate outcomes and final outcomes after the experiment ends. Table S18 shows the true expected final outcome $\tilde{\Psi}_{t,k}$ in ADAPT-R simulation.

Table S14: (a) True target estimand $\Psi_{t,k}$ had participants enrolled from $1, \dots, t - K$ been adaptively treated by a candidate adaptive design using surrogate Y_k in ADAPT-R trial simulations ($t = 11, 13, 15, 17, 19$). (b) Coverage probability (%) of confidence intervals for $\Psi_{t,k}$ in ADAPT-R trial simulations ($t = 11, 13, 15, 17, 19$)

(a) $\Psi_{t,k}$							(b) Coverage probability (%)						
t	$\Psi_{t,RCT}$	$\Psi_{t,1}$	$\Psi_{t,2}$	$\Psi_{t,3}$	$\Psi_{t,4}$	$\Psi_{t,5}$	t	$\Psi_{t,RCT}$	$\Psi_{t,1}$	$\Psi_{t,2}$	$\Psi_{t,3}$	$\Psi_{t,4}$	$\Psi_{t,5}$
11	0.538	0.542	0.540	0.538	0.538	0.538	11	95.8	95.8	95.2	95.8	96.4	95.8
13	0.547	0.557	0.552	0.551	0.549	0.547	13	96.0	96.2	95.8	95.6	94.8	95.6
15	0.557	0.570	0.567	0.564	0.562	0.560	15	94.6	95.4	94.8	94.8	94.2	95.4
17	0.562	0.578	0.575	0.572	0.570	0.568	17	95.0	95.4	95.6	95.2	95.2	94.8
19	0.564	0.579	0.576	0.574	0.572	0.570	19	94.0	94.8	96.0	94.6	94.6	94.8

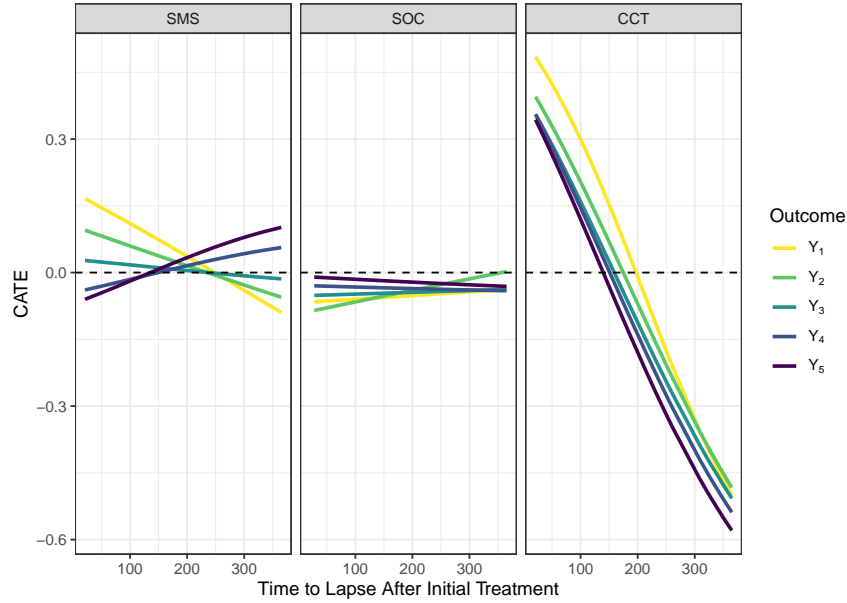


Figure S10: Estimated Conditional Average Treatment Effect (CATE) functions of Navigator v.s. SMS+CCT in Phase 2, plotted against initial retention strategy (grids) and time to lapse after initial strategy in Phase 1 (x-axis). Each curve corresponds to the CATE function of a candidate surrogate, ranging from Y_1 to Y_5 .

Table S15: Bias and variance of TMLE estimators for $\Psi_{t,k}$ in ADAPT-R trial simulations ($t = 11, 13, 15, 17, 19$).

(a) Bias ($\times 10^{-3}$)							(b) Variance ($\times 10^{-3}$)						
t	$\Psi_{t,RCT}$	$\Psi_{t,1}$	$\Psi_{t,2}$	$\Psi_{t,3}$	$\Psi_{t,4}$	$\Psi_{t,5}$	t	$\Psi_{t,RCT}$	$\Psi_{t,1}$	$\Psi_{t,2}$	$\Psi_{t,3}$	$\Psi_{t,4}$	$\Psi_{t,5}$
11	0.48	0.01	0.77	0.61	0.27	0.35	11	0.15	0.24	0.22	0.21	0.19	0.17
13	-0.30	-0.37	-0.32	-0.24	-0.60	-0.69	13	0.14	0.16	0.20	0.20	0.20	0.18
15	0.40	0.05	0.09	0.30	0.04	0.03	15	0.12	0.11	0.14	0.15	0.17	0.15
17	0.78	0.22	0.10	0.48	0.17	0.25	17	0.11	0.10	0.12	0.13	0.14	0.13
19	0.55	0.17	0.02	0.32	-0.06	0.10	19	0.10	0.10	0.11	0.12	0.13	0.12

J An Extension of the Proposed CARA Design

In some applications, when a plausible surrogate is available, experimenters may wish to adopt surrogate-guided adaptations before formally validating their utility for optimizing the final outcome. In such cases, a variant of TMLE-OSLAD can be used by designating a plausible surrogate (e.g., Y_k) as a primary outcome. The design then treats Y_k as the working primary outcome and updates treatment randomization probabilities as early as $t = k + 1$. As the experiment progresses, later surrogates can be promoted in sequence

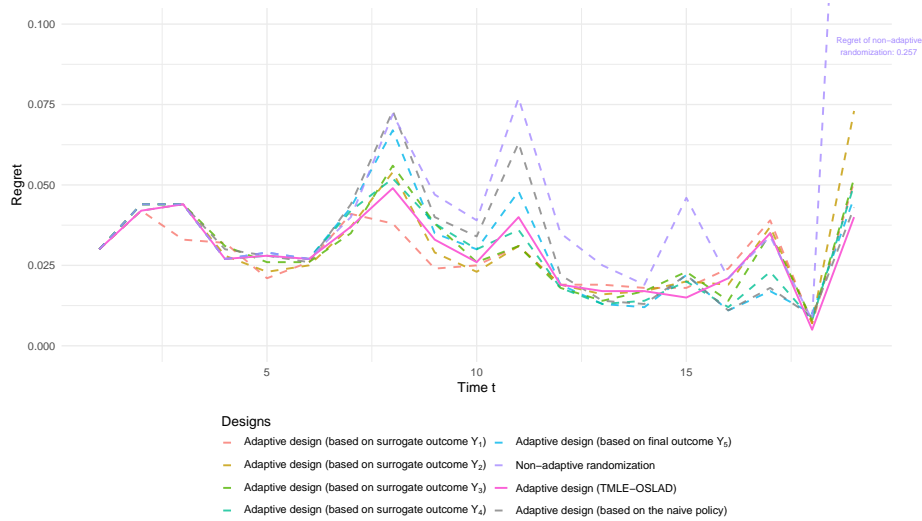


Figure S11: Regret at each time point t obtained from implementing different design strategies in the ADAPT-R trial simulation.

Table S16: Performance of TMLE estimators for adaptive-design estimands at the end of experiments in ADAPT-R trial simulation.

Estimand	Notation	Truth	Bias ($\times 10^{-3}$)	Var ($\times 10^{-3}$)	Coverage (%)
Expected final outcome under the adaptive design using Y_1	$\psi_{T_{end},1}$	0.581	0.36	0.09	95.4
Expected final outcome under the adaptive design using Y_2	$\psi_{T_{end},2}$	0.578	0.07	0.11	95.8
Expected final outcome under the adaptive design using Y_3	$\psi_{T_{end},3}$	0.576	0.33	0.12	95.4
Expected final outcome under the adaptive design using Y_4	$\psi_{T_{end},4}$	0.575	0.05	0.12	94.4
Expected final outcome under the adaptive design using Y_5	$\psi_{T_{end},5}$	0.573	0.31	0.12	95.2

as primary outcomes until the true final outcome Y_K is observed. If prior knowledge or external data may indicate the relationship between surrogates and the primary outcome, one may also initiate an earlier adaptation based on that information. However, these approaches typically rely on generalizability assumptions or pre-specified models of surrogate and primary outcomes. Regardless of the strategy chosen, the TMLE-OSLAD framework can be invoked throughout the experiment to evaluate the opportunities and costs of each candidate adaptive design and dynamically select the most useful one to support real-time decision making.

Table S17: Performance of TMLE estimators for other causal estimands at the end of experiments in ADAPT-R trial simulation.

Estimand	Notation	Truth	Bias ($\times 10^{-3}$)	Var ($\times 10^{-3}$)	Coverage (%)
Average treatment effect on the final outcome	$\psi_{n,5,T_{end}}^{ATE}$	-0.015	0.29	0.39	94.8
Expected final outcome under OTR of Y_1	$\psi_{d_{n,1,T_{end}}}^*$	0.591	0.45	0.13	95.2
Expected final outcome under OTR of Y_2	$\psi_{d_{n,2,T_{end}}}^*$	0.593	0.97	0.13	95.2
Expected final outcome under OTR of Y_3	$\psi_{d_{n,3,T_{end}}}^*$	0.593	1.36	0.16	94.0
Expected final outcome under OTR of Y_4	$\psi_{d_{n,4,T_{end}}}^*$	0.595	2.07	0.17	91.6
Expected final outcome under OTR of Y_5	$\psi_{d_{n,5,T_{end}}}^*$	0.592	1.11	0.21	92.8

Table S18: True expected final outcome $\tilde{\Psi}_{t,k}$ of implementing different designs in ADAPT-R trial simulation ($t = 11, 13, 15, 17, 19$).

t	$\tilde{\Psi}_{t,RCT}$	$\tilde{\Psi}_{t,1}$	$\tilde{\Psi}_{t,2}$	$\tilde{\Psi}_{t,3}$	$\tilde{\Psi}_{t,4}$	$\tilde{\Psi}_{t,5}$	$\tilde{\Psi}_{t,naive}$	$\tilde{\Psi}_{t,SL}$
11	0.538	0.542	0.540	0.538	0.538	0.538	0.538	0.538
13	0.547	0.554	0.551	0.551	0.549	0.547	0.546	0.551
15	0.557	0.570	0.567	0.563	0.562	0.560	0.558	0.564
17	0.562	0.575	0.573	0.571	0.570	0.568	0.565	0.571
19	0.564	0.577	0.575	0.573	0.572	0.570	0.567	0.573